Filopodial Activity of the Cardioblast Leading Edge in *Drosophila*

ANALYSIS OF CARDIOBLAST CELLULAR EXTENSIONS IN WILDTYPE AND MUTANT EMBRYOS DURING *DROSOPHILA* HEART DEVELOPMENT

By

QANBER SYED, B.Sc. (Hons.)

A Thesis submitted to the School of Graduate Studies

in Partial Fulfilment of the Requirements for the Degree

Master of Science

McMaster University

MASTER OF SCIENCE (2010) McMaster University
(Biology) Hamilton, Ontario

TITLE: Analysis of Cardioblast Cellular Extensions in Wildtype and Mutant Embryos during *Drosophila* Heart Development

AUTHOR: Qanber Syed, B. Sc. (Hons.) (McMaster University)

Supervisor: J. Roger Jacobs, Ph. D., Professor (McMaster University)

Co-Supervisor: Ana R. Campos, Ph. D., Professor (McMaster University)

Number of Pages: X, 88

Abstract:

The Drosophila heart arises from two bilateral rows of cardioblasts (CB) that migrate dorsally towards the midline and contact their contralateral partners to form the dorsal vessel. Generally, migrating cells rely on the extensions at the leading edge domain. Like other migrating cells, we show that the leading edge of the CBs extends finger-like processes which might play a role in sensing guidance cues during guided migration. Expressing an mCherry-Moesin transgene in the CBs enabled us to characterise the dynamic nature and genetic requirements of these filopodial processes. While studying the role of filopodial activity during heart assembly we observed that CBs extended cellular protrusions towards the internalizing amnioserosa cells. Filopodial activity is low during migration, and rises when the CBs are near the amnioserosa cells. However, filopodial contacts are stabilized by interaction with contralateral CBs, not the amnioserosa cells. CB cell bodies can contact their contra lateral partners only after the amnioserosa is fully internalized. We propose that filopodia are generated in response to the presence of sensory guidance molecules excreted by the amnioserosa cells.

Robo/Slit signalling has been previously shown to play a role in CB migration, adhesion and lumen formation. Additionally, studies have shown that Robo/Slit signalling plays a role in filopodial extension in the *Drosophila* nervous system development. We observed that in embryos in which Robo signaling in the CBs was reduced or absent, the CBs were less active at the LE. In addition, the migration speed of CBs in mutant embryos was notably decreased. Based on these results, we hypothesize that Robo/Slit signaling plays a role in filopodial extensions.

Acknowledgements:

I would like to thank my supervisor, Dr. Roger Jacobs for giving me a chance to work in his lab. By working under your supervision, I have learned many valuable scientific skills and also other valuable life skills which will help me become a better scientist. I would also like to thank Dr. Ana Campos, for all the advices which helped me become a more critical thinker and a better writer.

To the member of the LSB 420 crew, I want to thank you all for the support you have provided me. I would also like to thank Mihaela Georgescu for her great advices. To my fellow students, you guys have made my masters experience extraordinary and I will forever remember the unusual jokes and laughs we shared during our time spent together.

To my family members and friends, your support has helped me achieve one of my many goals. You guys are my inspiration and I hope to keep making you all proud.

TABLE OF CONTENT

LIST OF FIGURES **PAGE**

LIST OF TABLES

LIST OF ABBREVIATION

AS	Amnioserosa
cad	Gene encoding the cell adhesion molecule E-Cadherin
CB	Cardioblasts
CHD	Congenital heart disease
CNS	Central nervous system
DC	Dorsal Closure
DME	Dosral most ectodermal
dpp	Decapentaplegic
EGF	Epidermal growth factor
GAL4	Galactosidase transgene with 4 binding sites
kuz	Gene encoding the protein Kuzbanian
LE	Leading edge
LRR	Leucine rich repeats
RNAi	Ribonucleic acid interference
robo	Gene encoding the receptor Roundabout
sdc	Gene encoding the protein Syndecan
slit	Gene encoding the protein Slit
svp	Gene encoding the transcription factor Seven-up
TEM	Transmission electron microscope

tupGFP	Nuclear GFP marker under the control of the *tail-up* promoter
UAS	Upstream activating sequence

Introduction:

Many congenital heart diseases (CHD) are linked to developmental abnormalities that occur during heart formation (Hoffman. 1995; Bier and Bodmer. 2004). Since the underlying genetic mechanisms for these abnormalities remain unknown, it has been complicated to understand the exact causes of CHD. Because of consistent advances in genetic and medical technologies, many results from animal studies are being investigated in humans, and animal models such as zebrafish, mice and chick are proving to be substantial towards understanding human cardiac defects. However, a simpler organism, *Drosophila melanogaster,* has proved to be a strong model to study early heart development (Bier and Bodmer. 2004). Both classical and molecular genetics tools are applicable in this model to provide insight into heart cell specification and formation of a functioning dorsal vessel. In addition, various tools and short generation times allow us to evaluate genetic requirements for the formation of heart. Also, formation of the heart in *Drosophila* resembles early heart development in vertebrates (Bodmer and Venkatesh. 1998)(explored below). Therefore, studying genetic requirements and morphogenesis can contribute to the understanding of normal development and the development of CHDs. The general objective of this thesis is to better understand the genetic basis of the morphogenetic behaviours of Drosophila heart precursors.

The heart in *Drosophila*, also referred to as dorsal vessel, consists of cells which are organized in a tubular structure and pump hemolymph throughout the larval body. Even though the structure of the dorsal vessel does not bear a strong visual resemblance to the mammalian heart, many molecular mechanisms and morphological features are

conserved in both models (Bodmer and Venkatesh. 1998). Unlike invertebrate heart, the mammalian heart is looped and consists of multiple chambers with various cell types which play a specific role. In *Drosophila*, the heart is made up of a single tubular structure. Comparably, vertebrate's early development includes formation of a primitive tubular structure composed from the cells derived from the cardiac crescent (Chen and Fishman. 2000). Also, cells which will form the heart are derived from mesodermal precursors in both models (Bodmer and Venkatesh. 1998). However, due to the reversal of dorsal-ventral axis, the *Drosophila* heart forms dorsally whereas the vertebrate heart forms ventrally. Signalling pathways that regulate dorsal vessel formation are also conserved in vertebrates and include such pathways as BMP and Wnt signalling (Tao and Schulz. 2007). Additionally, structural and molecular similarities of the heart cells also exist in both models (Bodmer and Venkatesh. 1998).

During gastrulation, the invagination of the ventral furrow gives rise to mesoderm which then spreads laterally. Different stages of the embryogenesis are depicted in figure 1. Cardioblast (CB) precursors are specified from the mesoderm, specifically the dorsal mesoderm, by signals received from the adjacent ectoderm (Kadam, et al. 2009; Klingseisen, et al. 2009). Once the cardiogenic mesoderm is specified, ten clusters of paired cells are formed which will give rise to the dorsal vessel. These clusters of cells then collectively form a continuous row of CBs on each side of the embryo, adopt a cuboidal shape, and are perfectly aligned. At stage 13 these rows start to migrate dorsally towards the midline of the embryo along with the overlaying ectoderm. Once they reach the midline, contralateral CBs partners contact one another and lumen formation follows

(Tao and Schulz. 2007; Medioni, et al. 2008). By stage 17, the mature dorsal vessel formation is completed and synchronized contractions of the cells initiate.

1.1 *Drosophila* adult heart

The *Drosophila* larval heart is comprised of 52 contractile CBs on each side and surrounding pericardial cells. The muscular CBs are flanked by pericardial cells which are excretory cells in nature. Also, the CBs express muscle specific markers which are absent from the pericardial cells (Tao and Schulz. 2007). The Dorsal vessel can be divided into two domains which are morphologically different in larval heart. The anterior part of the heart, also known as the aorta, contains a narrow lumen which ends as the outflow tracts through which the hemolymph flows (Tao and Schulz. 2007). Posteriorly, the heart region contains a larger lumen and is able to contract more powerfully. This region is also referred to as the pump, since the contraction of this domain of dorsal vessel generates majority of the force which results in the circulation of the hemolymph around the larval body. The dorsal vessel is also segmentally patterned. In each segment of the heart, there are 6 pairs of cells. Two cells in each segment differ from the rest by the expression of the transcription factor *seven-up (svp)*. These cells are located at the most anterior part of the segment and will differentiate into the valves in the larval heart. The other four cells are *tinman* expressing cells and generally have larger nuclei compared to *svp* cells (Tao and Schulz. 2007).

Figure 1. **Dorsal vessel assembly.** The migration of the CB from the ventral mesoderm to the dorsal midline is shown below. (A) Lateral view of the embryo is shown at different stages of development, dorsal at top and anterior at left. During embryogenesis, cardiogenic precursors in the mesoderm are specified and from continuous bilateral rows of CBs (yellow) on each part of the embryo. Following germ band retraction, these rows start to migrate dorsally towards the midline. At stage 17, heart development is complete and synchronized contraction of the muscular heart follow. (B) Cross sectional images of the embryo are presented below at different stages of development. Cardiac precursor cells sit adjacent to the ectoderm and migrate along with the ectodermal leading edge. When the most dorsal ectodermal cells contact each other and dorsal closure is finished, cardiac cells contact each other and fusion of the CBs takes place. Figure adapted from Volker Hartenstein (Hartenstein, 2010).

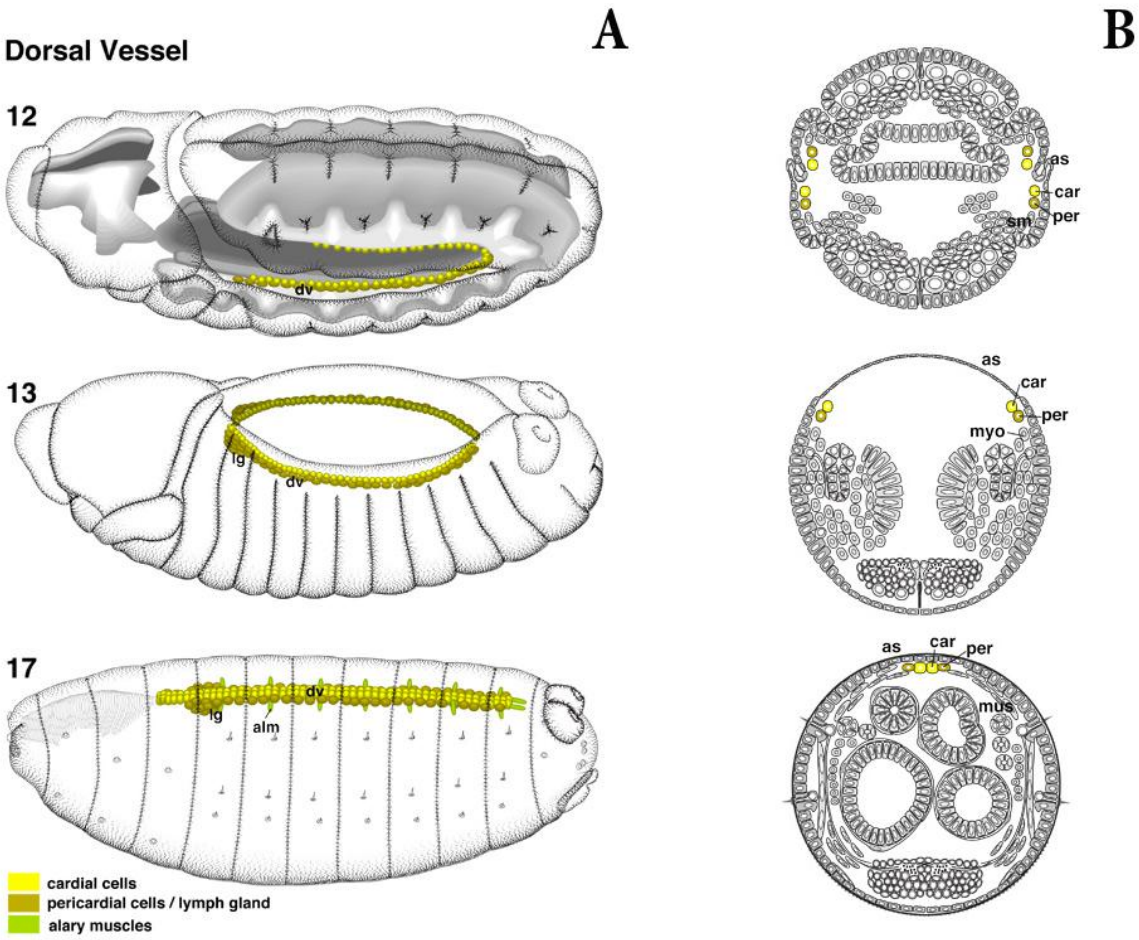
A
B
Dorsal Vessel
12
dv
13
lg
dv
17
dv
lg
alm
cardial cells
pericardial cells / lymph gland
alary muscles
as
car
per
sm
as
car
per
myo
as
car
per
mus

1.2 Dorsal Closure

Dorsal closure is a process during which the migrating ectodermal leading edge (LE) progressively covers the oval-shaped transient extra-embryonic epithelium called the amnioserosa (AS). The process occurs when the lateral epithelium from both sides of the embryo migrate dorsally over the exposed AS and fuse together to form a continuous epidermis (Heisenberg. 2009)(Figure 2). The ectodermal LE becomes active at stage 13, when cells begin to polarize and f-actin accumulates at the apical side of the cells (Jacinto, et al. 2002; Heisenberg. 2009). The organization of the LE cells also shifts from a scalloped edge into a straight continuous row of cells at this stage. Once the LE is established, migration of the cells begins. This migration is assisted by the mechanical forces generated during germ band retraction and later head involution (Kiehart, et al. 2000). This force assists in pulling the bilateral rows together towards the midline. The first contact that is made between the opposing bilateral rows is made between the most anterior and posterior part of the LE (Millard and Martin. 2008). Subsequently, dorsal closure progresses as the fusion of ectoderm spreads towards the center of the midline. Dorsal Closure also results in the internalization of AS (Hartenstein. 1992). Once the LE of ectoderm has come together the AS is internalized into the embryo at the dorsal midline. The internalization of AS occurs by constriction of the apical domain of the cells which eventually loses contact with the surrounding ectoderm (Scuderi. 2005). The AS then undergoes apoptosis.

Since the ectoderm is segmentally patterned, the recognition process across the midline has to occur accurately. These recognition events have been shown to be

filopodia dependent (Millard and Martin. 2008). Initially, the filopodia of the LE cells contact the opposing row. Normally, two recognition processes are responsible for proper dorsal closure. Compartments within the segments, anterior and posterior, are able to differentiate between one another by the activity of the filopodia (Millard and Martin. 2008). It was observed that, once the filopodia from one compartment contact the same compartment on the opposing row, the cells form stable filopodial contacts. Once the contact has been made between the same compartments of the segments, tethering of the filopodia between the cells pulls them together, which is proceeded by fusion (Millard and Martin. 2008). However, when filopodia from anterior compartment contact the filopodia of posterior compartment on the opposing row, stabilized interaction is not observed. One interesting observation is that anterior and posterior compartment cells are capable of stabilizing contacts with their respective cells even when they are located within a different segment. When this occurs, the segmental boundaries are interrupted and dorsal closure halts. Also, in some cases the epithelial sheets poorly align along the midline. In such cases it was observed that filopodia are able to identify and contact correspondingly matching cells which are several cell diameters away. Once again the contraction of the filopodial tether pulls the cells towards one another and realigns the entire segment correctly (Millard and Martin. 2008). This data demonstrated that not only do filopodia play a role in sensory guidance, but also are able to contract and draw matching cells together.

Figure 2. Ectodermal and CB Leading Edge. (A-D)Dorsal view of the *Drosophila* embryo undergoing dorsal closure is shown below. As the germ band retracts the LE of the ectoderm is stretched and aligns into continuous rows of cells on each side of the embryo. (B) The LEs then migrate towards the midline. As the rows meet each other at the midline, zippering of the ectoderm takes place. (C) The extraembryonic tissue, amnioserosa, is internalized into the embryo as the ectoderm fuses together. (D) At the end of dorsal closure, a continuous epidermis covers the dorsal hole. (E-F) Fixed transmission electron microscope image showing cross sectional view of the *Drosophila* embryo is presented below. (E) At stage 15, CBs extend processes at the apical side of the cell and assume a pear shaped morphology as they get closer to the midline. CBs physically interact with ectodermal LE cells and internalizing AS cells. (F) By stage 16, CBs are closer to the midline and extend cytoplasmic processes over the internalizing AS cells. Once the ASl cells have lost contact with the ectoderm, CBs are able to contact their contralateral partner cells and fusion of the cells proceeds. Adapted from Antonio Jacinto, 2002., Panels E,F from R. Jacobs.

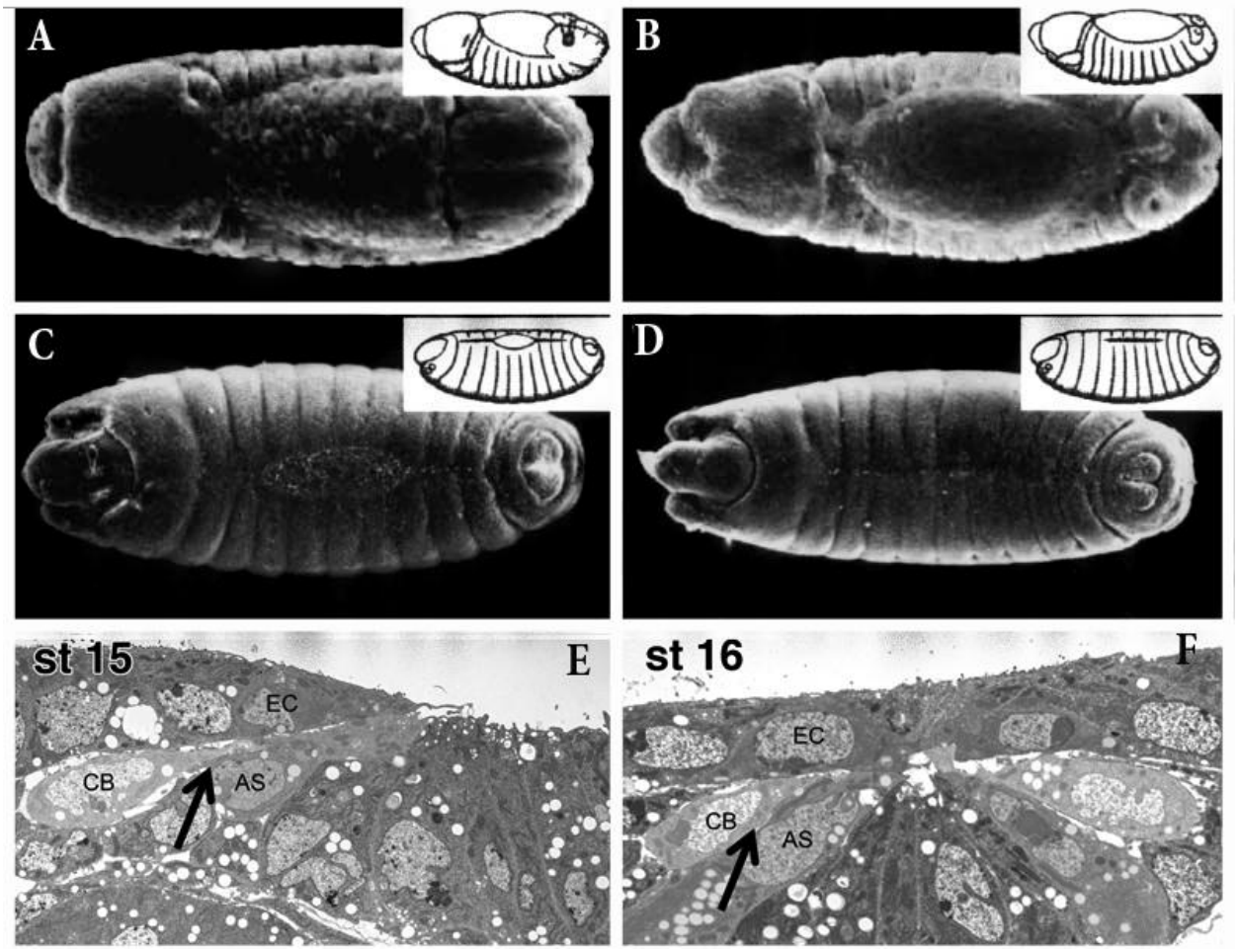
A
B
C
D
st 15
E
EC
CB
AS
st 16
F
EC
CB
AS

Furthermore, the sensory role of filopodia has been demonstrated in several model systems (Millard and Martin. 2008; Kohsaka and Nose. 2009; Tucker, et al. 2011). One of these models is neuromuscular synapse formation in *Drosophila*. During the formation of muscle synapse, the pre-synaptic neuron extends filopodial processes which contain guidance-related proteins at their tips (Kohsaka and Nose. 2009). Often, the distal part of the Filopodia is responsible for making the initial contact with the target cell. Study conducted by Kohsaka provides evidence that postsynaptic filopodia are able to perform a sensory function and protein-mediated recognition is involved in synaptic matching (Kohsaka and Nose. 2009). Signalling and adhesion molecules also tend to concentrate at the tips of the filopodia (Edwards, et al. 1997; Kohsaka and Nose. 2009). Hence, filopodia are believed to participate in the recognition of guidance cues and target cells.

1.3 Cellular interactions of cardioblast and ectodermal leading edges

Interactions between cells that occur through direct contact play an important role in specifying fate and function of cells in many organ systems. Not only direct contact but signalling via soluble factors also contributes to morphogenesis. Many attempts have been done to create an *in vitro* system in which the cells maintain their identity outside of their normal environment. However due to the lack of complex micro-environmental interactions which are found *in vivo*, survival of the cells in these systems is not guaranteed. Even though several technologies exist which have been successful in replicating *in vivo* environment in an *in vitro* model, not all cells are capable of growing in such conditions and require complex interactions with surrounding tissues. Therefore, creating a new *in vivo* method to study cell-cell interaction is of interest.

One of the models developed in *Drosophila* to study cell-cell interaction is the muscle synapse formation during embryogenesis (Keshishian, et al. 1996). In this model, pre-synaptic neurons migrate towards the post-synaptic muscle fibers and form synapse once the contact has been established. This model has helped in discovering proteins that are involved in cell recognition and also signalling molecules that attract the cells together (Kohsaka and Nose. 2009). Dorsal vessel formation also serves as a model for studying cellular interactions. First, the CB migrate and must contact their contralateral partners. Furthermore, since CBs migrate along with the ectodermal LE, it was hypothesized that physical interaction between the two cells existed. TEM cross-sectional images of the *Drosophila* embryo are depicted in figure 2 (MacMullin and Jacobs. 2006). At stage 15 it is observed that CBs extend cytoplasmic processes towards the midline. In addition, CB processes seem to directly contact both the most dorsal most ectodermal (DME) cell and the internalizing AS cells. Also, the extension of the processes is concentrated between the ectodermal cells and the AS cells. At stage 16, CBs make their way closer to the midline. Dorsal closure is completed at this stage and the AS cells occupy the midline position right below the ectoderm as seen in figure 2. CB further extend processes toward the midline in search of their contralateral partners (Fig 2E-F, arrow) (MacMullin and Jacobs. 2006). At this stage direct physical interaction between both AS and ectodermal cells are observed. In fact, in fixed embryos AS cells contact CBs at the luminal domain (explored below), which is the domain that will encompass the lumen.

Cell-cell interactions are also observed during the migration of ectodermal LE and AS internalization (MacMullin and Jacobs. 2006; Millard and Martin. 2008). First the LE cells interact with the AS cells. Subsequently, LE cells interact with the opposite row and undergo fusion to form a continuous ectoderm. AS cells on the other hand are internalized and undergo apoptosis (Toyama, et al. 2008). After the fusion of the ectoderm, AS cells still maintain contact with the ectoderm (Niloufar Mohseni, Reed personal communication). Apoptosis in AS cells occurs due to the loss of apical contact of AS cells with the dorsally located ectoderm (Nilufar Mohseni, Reed personal communication). However, not only is apoptosis a way to eliminate unwanted cells, in some cases it also serves other functions, one of which is the releasing of signalling molecules by which contribute to changes in the micro-environment (Poelmann and Gittenberger-de Groot. 2005). This indicates that tissues surrounding apoptotic cells might be affected by direct contact or by signalling molecules released from the cells and responds correspondingly (Poelmann and Gittenberger-de Groot. 2005).

Preliminary experiments suggested that CBs contact the internalizing (apoptotic) AS cells at later stages (figure 2E,F). However, at stage 15 when the CBs are far apart from the midline, apoptosis is already triggered in AS cells that have been internalized and have lost contact with the ectoderm. Interestingly, the presence of these apoptotic cells coincides with the location where the future dorsal vessel is going to form. Since CB must travel towards the AS cell (midline), it might be possible that the CB migration is instructed by guidance molecules originating from the apoptotic AS. On the other hand, the ectodermal LE cells are also observed to directly contact the CB at late stages. It has

been shown that ectoderm specifies the fate of mesodermal cells to dorsal mesodermal cells via a secreted protein, Decapentaplegic, which activates the signalling pathways in target cells (Tao and Schulz. 2007). These cells will then be further specified to CBs via another signalling pathway activated by *wingless*, which is expressed and secreted by the transverse stripes of the ectoderm (Tao and Schulz. 2007). Therefore close proximity of mesodermal cells and their interaction with ectoderm at very early stages serves a crucial role (Zaffran and Frasch. 2002). That being said, the interaction at later stages with surrounding cells, direct or via signalling molecules, might also be required to further specify domains or localize certain proteins at the membrane of CBs.

1.4 Slit/Robo signalling

The *roundabout (robo)* gene was initially identified in *Drosophila* (Seeger, et al. 1993). There are three homologues of *robo* in *Drosophila (Robo-1, Robo-2* and *Robo-3),* whereas, in vertebrates four Robo homologues are present. The role for Robo was discovered initially in commissural axons in the *Drosophila* nervous system (Seeger, et al. 1993).The ligand for Robo, Slit, was first identified as a protein secreted by the midline glia (Rothberg, et al. 1990; Battye, et al. 1999) . Binding of Slit to Robo activates Robo signalling and transduces a repellent signal which specifies the positioning of axon tracts. This prevents axons from crossing the midline and is required to form the ladder-like structure of axon bundles in the CNS (Brose, et al. 1999; Dickson and Gilestro, 2006).

Slit is a secreted glycoprotein which has an N-terminal signal peptide, four leucine –rich repeat domains (LRR) at the N-terminus termed D1-D4. This is followed by six EGF-like domains, a laminin-G like domain and a C-terminal cysteine knot (Kidd, et al.

1999; Hohenester. 2008). Slit is naturally cleaved into a short C-terminal fragment, for which the function is unknown. The cleavage also results in the production of a long N-terminal fragment which binds to Robo and can actively promote Robo signalling (Brose, et al. 1999). Robo, however, consists of five Ig-like domains which are followed by three fibronectin type 3 domains (Hohenester. 2008). The cytosolic domain of Robo has shown to have four conserved cytoplasmic sequence motifs which have been named CC0-CC3 (Kidd, et al. 1998; Hohenester, et al. 2008). They are thought to be binding sites for various cytoplasmic adaptors proteins such as Ena/VASP proteins and Rho family GTPase activating proteins, which convey signalling downstream (Bashaw, et al. 2000). It is not clear whether these signalling pathways act together or separately to repel axons in the CNS. Interestingly, it has been noted that some Robo's do not have all of the four CC motifs. For example, vertebrate Robo lacks CC1, *C. elegans* Robo lacks CC0 and CC3, whereas the Drosophila Robo2 and Robo3 lack CC2 and CC3 domains (Hohenester, 2008). This indicates that even though Robo's extracellular domains are identical, differences in the cytoplasmic domain structure might result in binding of different adaptor proteins.

Mutagenesis studies suggested that second LRR domain (D2) of Slit binds to the Ig domain on Robo and recently biochemical studies have confirmed that indeed D2 domain of Slit binds to the first Ig domain of Robo (Liu, et al. 2004). Further, the interaction between Robo and Slit is enhanced by a heparin sulphate proteoglycan, Syndecan. It has been shown that Sdc can interact with Slit and Robo and its activity contributes to the repulsion of the axons at the CNS midline. Studies in *Drosophila* have

shown that Sdc regulates the efficiency and distribution of Slit. The Precise function of Sdc in Robo signalling is unknown; however, it is thought that a formation of a ternary complex takes place where Sdc assists in Slit-Robo binding (Johnson, et al. 2004). Also, it has been shown that Sdc is required for proper lumen formation and requires apicalization of the Slit-Robo complex (Knox, et al. 2011).

The function of Slit and Robo has also been identified in other developmental processes including the morphogenesis of the salivary gland and trachea (Englund, et al. 2002; Kolesnikov and Beckendorf. 2005). During salivary gland development, presence of Slit in the CNS repels the salivary gland lobe away from the midline. In *slit* mutants, salivary glands extend their lobes towards the CNS (Kolesnikov and Beckendorf. 2005). In trachea development, it has been shown that Slit can act as both an attractant and repellent (Englund, et al. 2002). In the absence of *robo-1*, ganglionic branches mistakenly cross the midline, which suggests that *slit* signalling via this receptor mediates a repulsive signal. However, in the absence of *robo-2*, ganglionic branches fail to enter the CNS (Englund, et al. 2002). This suggests that Robo2 may mediate an attractive signal and differs from the function of Robo-1. In addition, overexpression studies of Slit in the gut showed that only Robo-2 is able to mediate an attractive response to Slit (Englund, et al. 2002). The study also demonstrated that a signal mediated by Robo-1 is antagonistic to signalling via Robo-2 (Englund, et al. 2002).

Another signalling system which serves an antagonistic function to Slit-Robo signalling is signalling via Frazzled by its ligand Netrin. In this model Netrin serves as a midline attractant during CNS development (Bashaw and Goodman, 1999; Harris, et al.

1996). One study was conducted to test the nature of the cytoplasmic domain of both robo and frazzled receptors. Chimeric receptors were generated in study and subsequent effects of the expression of these receptors were tested by either Netrin or Slit (Bashaw and Goodman, 1999). When an ectodomain of Fra and cytoplasmic domain of Robo were linked, Netrin served as a repulsive signal. However, when the domains of receptors were switched, Slit served as an attractive signal (Bashaw and Goodman, 1999). This observation indicates that depending on the receptor structure, specifically the cytoplasmic domain, the attractive or repulsive nature of the guidance molecules is exposed.

1.5 Lumen formation in the dorsal vessel

Once the bilateral rows of CBs have met at the dorsal midline, lumen formation proceeds. Even though the typical model for lumen formation involves deformation of an already present apical surface, the current model of lumen formation differs in the *Drosophila* heart. First the dorsal apical part of the CBs makes contact with the equivalent domain on its contralateral partner (Medioni, et al. 2008). Once the contact is stabilized, the ventral-apical domain of the cell extends cytoplasmic protrusions which contact the equivalent domain of the partner cell. This process creates a hollow space at the center of the cell which serves as the lumen (Medioni, et al. 2008).

For the generation of the lumen, specific adhesive and de-adhesive forces are required along the apical side of the CBs. The de-adhesive forces have to be generated at the central domain of the cell, whereas the most dorsal and ventral domain must adhere to one another. As in nervous system, Slit and Robo here act together to form repulsive

forces between the luminal domain of the CBs (Medioni, et al. 2008; Santiago-Martinez, et al. 2008). In loss of function *slit* and *robo* mutant embryos, absent or reduced lumen phenotypes are observed. Slit is secreted by the CBs and as the development progresses, changes its uniform plasma membrane localization precisely to the apical domain (MacMullin and Jacobs, 2006). Robo localization also becomes more apical, specifically at the central domain of the cell and not the dorsal-apical and ventral-apical domains (Santiago-Martinez, et al. 2008). This observation further indicates the role of Robo and Slit in lumen formation.

In contrast to repulsive forces, adhesive forces are required at the dorsal- and ventral-apical domains. These forces are generated by the homophilic interaction between DE-Cadherin (Santiago-Martinez, et al. 2008). Generally, the localization of DE-cadherin is specific to the dorsal-, ventral- apical domains (Junctional domain) (Santiago-Martinez, et al. 2008). In *E-cadherin* mutants, the cells are able to align at the midline, however there is no adherence between the cells (Medioni, et al. 2008). In these embryos, lumen also fails to form. In contrast, in *robo* mutants, DE-cadherin localization is observed along the entire apical domain of the CBs (Santiago-Martinez, et al. 2008). This results in formation of adhesive forces between DE-cadherin and hence no lumen is formed. Therefore, the presence of Robo at the luminal domain restricts DE-cadherin localization to the dorsal- and ventral- apical domains.

1.6 Kuzbanian function during embryogenesis

Notch signalling plays important roles at different stages of cardiac development. A critical step in Notch signalling is the activation of Notch receptor which leads to the cleavage of the intracellular domain of the receptor. This cleavage product serves as a transcription factor and activates the expression of downstream genes. Notch receptor cleavage is achieved by ADAM metalloproteases (Lieber, et al. 2002; Zhang, et al. 2010). The homolog of this protease, *kuzbanian (kuz),* was first identified in *Drosophila* and has been shown to cleave the S2 site of the Notch receptor (Rooke, et al. 1996; Albrecht, et al. 2006). Kuz is a transmembrane protein and is expressed throughout development in the CNS. Kuz mediated cleavage is not limited to Notch receptor but also cleaves amyloid precursor protein and ephrins (Albrecht, et al. 2006). Interestingly, Kuz plays a role in axon guidance as well (Rooke, et al. 1996). When a dominant-negative form of Kuz was expressed in the midline glia cells midline axon repulsion was disrupted and crossing of ipsilateral axons took place (Coleman, et al. 2010). A study published by Bashaw and colleges, indicated that Robo cleavage is promoted by the activity of Kuz (Coleman, et al. 2010). In addition, overexpression of an uncleavable robo construct does not rescue *robo* mutant phenotype. Therefore, kuz based cleavage of Robo receptor is crucial for proper midline axon repulsion.

In dorsal vessel development, Kuz has been shown to play a role in Notch-based lateral inhibition (Albrecht, et al. 2006). In *kuz* mutants, a hyperplasic heart is formed, in which the number of CBs is almost doubled. Both *tinman* and *svp* expressing cells were affected in these mutants. In addition to duplication of cells, phenotypes such as

uncoordinated arrangement and multiple lumens were observed (Albrecht, et al. 2006). This suggests that, other than early stage cleavage of Notch, Kuz plays an additional role in cell morphogenesis. Due to a genetic interaction between *kuz* and *robo* in the CNS (Coleman, et al. 2010), it might be possible that cytoplasmic domain of Robo is a cleavage substrate for Kuz in heart development as well.

1.7 Hypothesis and Objectives

CB and the ectoderm LEs behave similarly in many ways. For example, both of the Les (Ectodermal and CB) migrate together; both LEs travel towards the midline and fuse with specific partner cells localized to the opposing row. Therefore, I hypothesize that CB are associated with the ipsilateral ectodermal LE and migrate synchronously to the dorsal midline. I hypothesize that CBs are capable of extending filopodial processes similar in behaviour and function to those observed in ectodermal LE cells. Also I hypothesize that CB filopodial processes contact the ectoderm and internalizing AS. Lastly, Slit/Robo signalling has been implicated to play a role in cytoskeletal rearrangement (Ghose and Van Vactor, 2002). Since axon repulsion during CNS development requires cytoskeletal remodelling which is required for the diversion of axons, it is possible that Robo signalling might play a role in cytoskeletal rearrangement. Therefore I hypothesize that filopodial activity might be affected when Slit/Robo signalling is down regulated. To test these hypotheses following objectives were stated:

Primary Objectives

1) Asses the activity of the LE in the CB
    a. Assess the behaviour of CB filopodia while focusing on contact between contralateral and non-contralateral partner cells
2) Study the interaction between CBs and surrounding tissue, such as the AS and ectoderm.
3) Explore the role of Slit/Robo signalling in CB LE filopodial extension
4) Study the effects of *kuzbanian* down regulation in late stage dorsal vessel development and filopodial extension

Chapter 2

MATERIALS AND METHODS

2.1 *Drosophila melanogaster* strains

The *UAS-moesin-mCherry* stock was provided by T. Millard (Development (2008) 135, 621-626). *tupGFP* stock was provided by R. Schulz (University of Texas, Houston). *svpGAL4* stock was provided by R. Cripps. *dmefGAL4* stock was provided by C. Goodman. *svpGAL4*, *tupGFP* recombinant stock was created by C. Soldaat (McMaster University, Hamilton). AS markers and drivers were provided by B. Reed (University of Waterloo, Waterloo). All RNA interference lines, *UAS-Slit-RNAi* (20210) and *UAS-Cadherin-RNAi* (27081)*;* were obtained from Vienna *Drosophila* RNAi Center. *Slit*^{2}, *robo*^{1}and *UAS-Kuzbanian-DN* stock were obtained from Bloomington *Drosophila* stock center. UAS-Syndecan-GFP was provided by G. Vorbrüggen (Institute of Biochemistry, Zürich). *UAS-triple-Robo-RNAi* was provided by G. Bashaw (University of Pennsylvania, Philadelphia).

2.2 Embryo collection and hanging drop mounting method for time lapse imaging

Initially, the flies were placed inside a house (100ml beaker with holes at the top) with a 60 mm apple juice agar plate at the bottom. For optimal egg laying, a small amount of yeast paste was added to the agar plate and the houses were kept at room temperature. The agar plates were placed in the house in the evening and then changed in the morning prior to embryo mounting.

The protocol for mounting embryos is described at Jove by B. Reed (Reed, et al. 2009). A custom made observation chamber was used for live imaging. The chamber contains a depression in the middle on top of which the cover slide is placed. A moist tissue was placed inside the depression of the chamber to keep the embryos hydrated. The embryos were handpicked using forceps from the agar plate and placed on the slide on which double sided tape was adhered. With the use of a Nikon dissecting microscope and forceps, the embryos were manually dechorionated and placed onto a 22 x 40 mm #1 cover slip. A single drop of oxygenated halocarbon oil was then placed immediately on the embryo to prevent dehydration and hypoxia. Embryos were then oriented dorsally facing downwards towards the coverslip. In similar manner, several embryos were usually placed on the coverslip prior to imaging. The coverslip containing the embryos was then placed on top of the observation chamber so that the embryos are hanging into the depression towards the moist tissue. The embryos were also oriented to face dorsally upwards (towards the cover slide). Tape was applied to the sides to secure the cover slip on top of the chamber. The observation chamber was then carefully carried to an upright confocal microscope.

2.3 Time lapse imaging

CB migration was documented using the Leica TCS SP5 upright confocal microscope. Time lapse movies and images were acquired using Leica LSM software. All movies were filmed using a 60x objective with oil immersion coating for high resolution images. Zoom was adjusted depending on the type of experiment (1x for dorsal view movies, 2.5x for cross-section movies and 3x for high magnification images). Depending

on the stage of the embryo, z-stacks were obtained spanning from 15µm up to 30µm and merged at the end of imaging. The pinhole was adjusted to 145µm, hence each z-section was 1.5µm in depth. The distance between the z-stacks was 1µm for frontal movies and 0.5µm for cross-sectional movies. For green channel imaging, Argon laser was adjusted to 17% of full power. For imaging in red channel, HeNe 594nm laser was used at 60%. Gain was adjusted differently for each embryo to obtain suitable images. Depending on the experiment, images for movies were taken with various intervals (1 frame per minute for frontal movies and continuous scanning for high magnification images). In addition, the blur function was applied to final movies to reduce background noise. Color adjustment was applied to both green and red channels using Adobe Photoshop. Final movies were saved in .avi format.

2.4 Measurement of leading edge activity

Measurements for LE activity were performed using ImageJ software. The Set Scale tool was used to convert size of pixels into micrometers by drawing a line across the scale bar and defining the length of the scale bar. The software then memorized the ratio of pixels to micrometers and gave the final measurements in micrometers. To measure the percentage activity, the total lengths of bilateral rows on each side were measured by drawing and measuring a line along the apical surface of the cells. Subsequently, active parts of the LE were identified by the presence of cellular extensions which were extended away from the cell. These cellular extensions were identified by comparing the difference between the z-stacks recorded at the dorsal and ventral apical domains. A line was drawn from the center of CB nuclei to the tip of the furthest

cytoplasmic extension at the dorsal-apical domain. Same measurement was performed for the luminal and ventral-apical domain. If the distance from the CB nuclei to the tip of cytoplasmic extension differed between the domains, LE was measured to be active. If the difference in the measurement was approximately identical between the domains then those cells were deemed unactive. Once the active parts were identified, the lengths of active membrane were measured by drawing and measuring a line across the apical membrane of the active cells. Length of active LE was then obtained by summing the length of apical membrane in active cells separately for each bilateral row. Ratios for LE activity were obtained by dividing the cumulative length of active LE cells over the total length of LE and multiplied by 100 to obtain a percentage.

2.5 Measurement of CB migration speed

Migration speeds were calculated using ImageJ software. Time-lapse movies were used in which CB migration was documented. By looking at the first and last frame of the movie, migration pattern and distance covered by the CB was measured in μm. This was done by drawing a line, starting from the center of the nuclei, from its initial location to the final location. This line was measured and represented the distance covered by the CB. Based on the number of frames in the dorsal view time-lapse movie (1 frame per minute), time it took for CB to reach from initial point to final point was measured. Speed was obtained by dividing distance covered by CB over time; it took for the completion of migration (μm/min).

CHAPTER 3: Results

3.1 Leading edge of cardioblasts extends finger like filopodial processes

During cell migration, the orientation of the LE dictates the direction of the movement. The movement is assisted by the cellular processes, such as filopodia and lamelopodia, which are present only at the LE. Localization of molecules important for target recognition, sensory guidance and adhesion molecules are all shown to be present on the LE and play important roles in the migration (Galbraith, et al. 2007; Kohsaka and Nose. 2009). Therefore, observing the basic behaviour of the cellular processes in migrating cells is important. Previously, filopodial processes in the ectodermal LE have been visualized using a *moesin*-mcherry tagged construct (Jacinto, et al. 2002; Millard and Martin. 2008). In order to visualize filopodial processes in the migrating CBs, I drove the expression of UAS-*moesin*-mcherry construct using a GAL4 transgene under the control of a cloned enhancer of myocyte enhancer factor-2 (MEF-2). This transcription factor is muscle specific and since cardiac cells are muscular in nature, the expression of the *moesin-mcherry* construct was achieved in CBs. Also to differentiate between contralateral and ipsilateral partners, a *tupGFP* construct was also expressed in the embryos which labelled the nuclei of all CBs.

Wild-type embryos expressing both *tupGFP* and *moesin-mcherry* were observed using live imaging and time lapse movies were recorded. Due to the apparent bleaching of the mcherry tag by the HeNe 594 nm laser, I was unable to produce single movies which encompass the entire dorsal vessel development. Since the development of the dorsal vessel proceeds for approximately 2.5-3 hours, several forty minute movies were

made so that all of the developmental stages were included in the recording. CB LE was observed to extend cellular processes from the apical side of the cells (Fig 3). The filopodial and lamellipodial processes varied in length and appear to be present on surface of some specific cells (Fig 3E, asterisks). We also observed that CBs are able to extend multiple filopodial processes per cell (Fig 3F).

At early stage 15, when the bilateral rows have not made contact, filopodial activity was low. At this stage the anterior and posterior cells of the bilateral rows appeared to be more active (Fig 3A, arrow) compared to the cells localized to the central region of the rows (Fig 3B, arrow). As the bilateral rows came within close proximity to one another at late stage 15, the presence of filopodia on the anterior and posterior cells increased significantly, whereas the centrally localized cells still maintained a low or no level of filopodial activity (Fig 3B,arrow). At late stage 15, most posterior and anterior cells were first to make contact and start forming adhesions with their respective contralateral partner cells (Fig 3C, arrows). Some cells in the LE appeared to be more active than their neighbours (Fig 3E, asterisk).

To test whether the increase in filopodial activity is directly proportional to the distance to the midline we measured the overall activity of the LE at different stages of development. At early stage 15, we observed that the median percentage of active LE was 40% (Table 1). For the LE activity calculation, refer to the methods and material section. This activity increased to 70% by stage 16. At late stage 16, when most of the anterior and posterior cells have fused with the partner cells, the centrally located cells of the LE were fully active. Since the activity of the LE appears to increase as the distance between

CB decreases, a scatter plot was constructed to observe this correlation (Fig 5). Based on the scatter plot, it appears that there is a direct correlation ($r = -0.60$) between the distance of cells to the midline and LE activity.

Figure 3. Cardioblasts extend filopodial processes. (A-D) Complete heart images from time lapse movies of *dmefGAL4, tupGFP, UAS-moesin-mcherry/+* embryos expressing *tupGFP* (green) and *moesin-mcherry* (red) are shown. (A) At early stage 15, LE is not active. However the posterior cells on the bilateral row (arrow) were observed to extend finger-like cytoplasmic extension. (B) At late stage 15, more posterior and anterior cells became more active as they got closer to the midline. The centrally located cells did not show increased filopodial activity. Nevertheless low basal filopodial activity was present in these cells (arrow). (C) At stage 16, activity of the entire LE increased significantly and fusion between the most anterior and posterior contralateral partners occurred (arrows). (D) At late stage 16, central cells made contact and eventually all of the cells fused together and lumen formation proceeded. (E-H) High magnification images from time-lapse movies of embryos expressing *moesin-mcherry* are shown. (E-F) The aorta portion of the heart is shown at stage 15 (E) and stage 16 (F). LE in the aorta and heart was highly active with filopodia extending and retracting constantly. Average filopodial extension time was measured to be 123s in the aorta region (n=20) and 176s in heart region (n=20). Bifurcation (arrow) of filopodia were also observed (arrow). Filopodial contact occurring between non-contralateral partner cells was observed (arrow head). However, this contact did not stabilize (arrows). Once the bilateral rows were in close proximity to the midline, some CBs appeared to be more active compared to neighbouring cells (asterisks). Intensity of the red and green channels was adjusted in these and all subsequent images. Anterior of the embryo in all images is to the left.

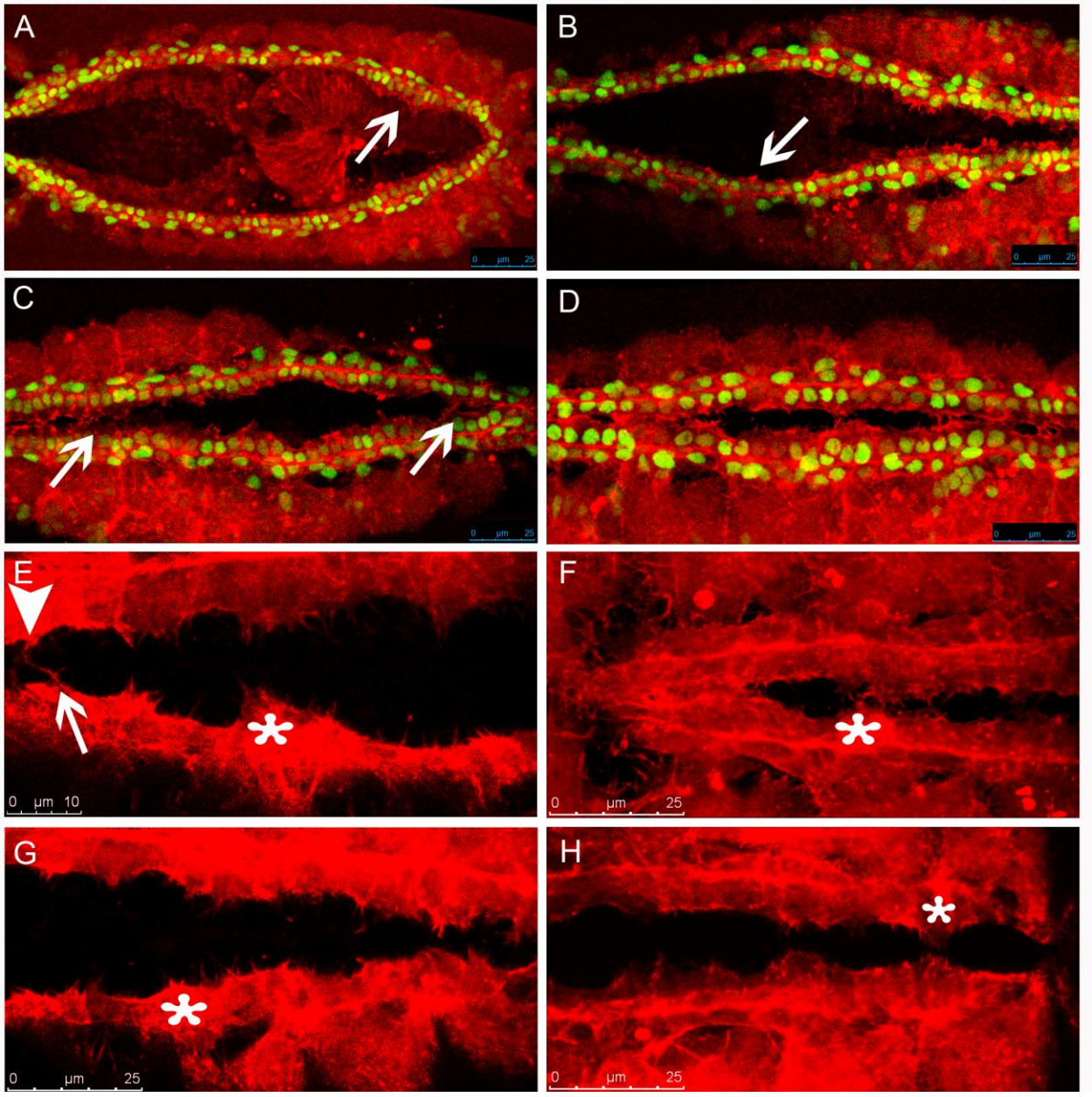
A
B
C
D
E
F
G
H
0 µm 10
0 µm 25

Figure 4. Filopodia contact non-contralateral partner cells. Images from high magnification time lapse movies are shown below. The images show the behaviour of filopodia and how the contact is achieved between non-contralateral partner cells. Single filopodial contact is shown below (arrows) between non partner cells at the aorta region of the heart. The contralateral partner cells on each row were identified by looking for the formation of the stable contact at the end of the movie. Contralateral partner cells nuclei are marked with asterisks. Once the cells were identified as contralateral partners, they were marked and tracked back to the beginning of the movie. The filopodial contact did not result in formation of stable contact between the cells and was observed to disappear by the end of the time lapse movie.

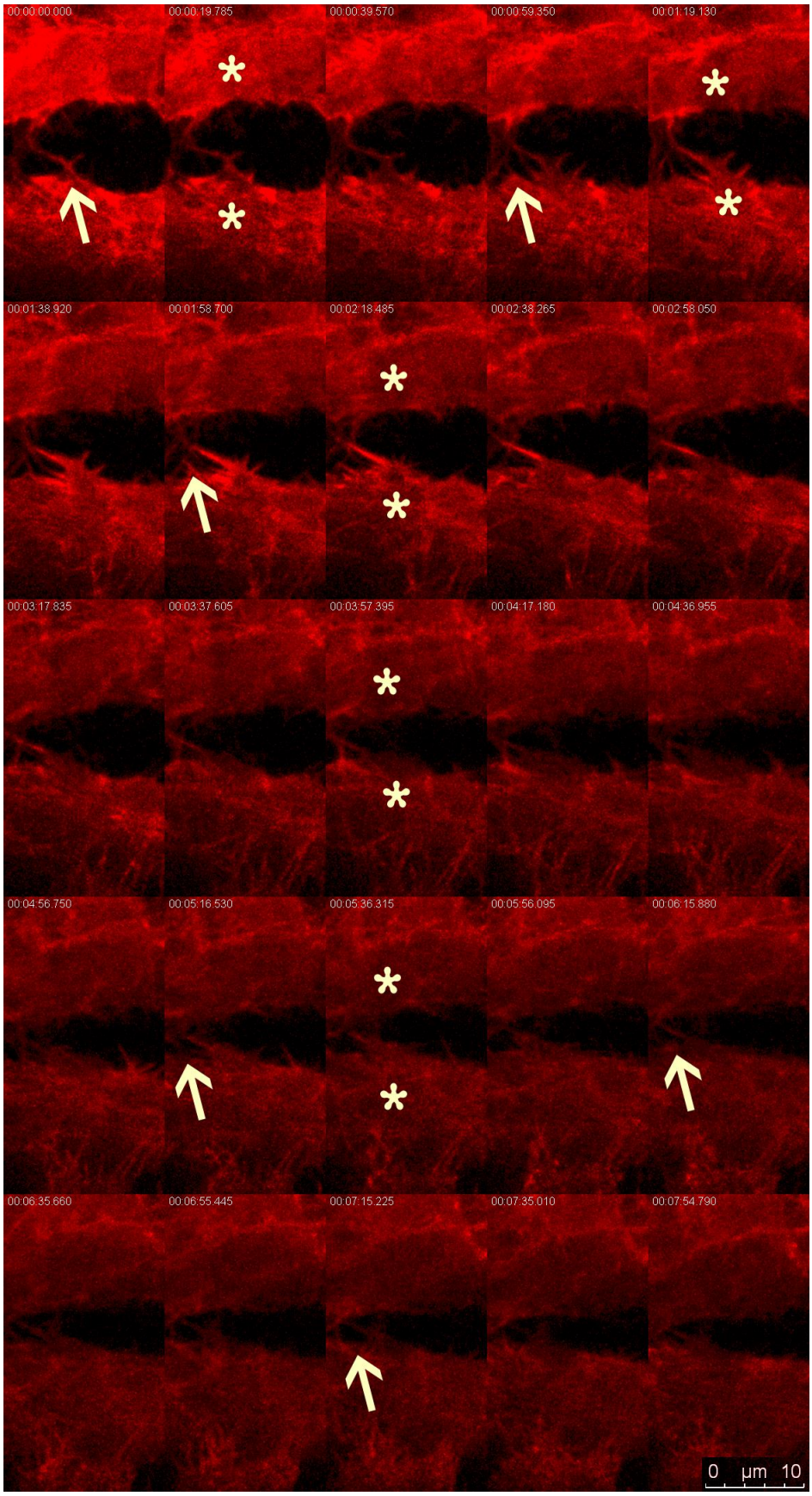
00:00:00.000
00:00:19.785
00:00:39.570
00:00:59.350
00:01:19.130
00:01:38.920
00:01:58.700
00:02:18.485
00:02:38.265
00:02:58.050
00:03:17.835
00:03:37.605
00:03:57.395
00:04:17.180
00:04:36.955
00:04:56.750
00:05:16.530
00:05:36.315
00:05:56.095
00:06:15.880
00:06:35.660
00:06:55.445
00:07:15.225
00:07:35.010
00:07:54.790
0 µm 10

Figure 5. Scatter plot of distance between the most central CB and midline vs Percentage activity of the leading edge. The graph shows how the distance of CB to the midline influences the filopodial activity of the LE. The X-axis represents the distance from the most central CB nuclei of the bilateral row to the midline. The Y-axis represents the percentage activity of the LE. A trend emerges from the data and indicates that as the distance between the most centrally located cells on the bilateral rows decreases, the activity of the LE increases. 13 LEs were used for the generation of the graph.

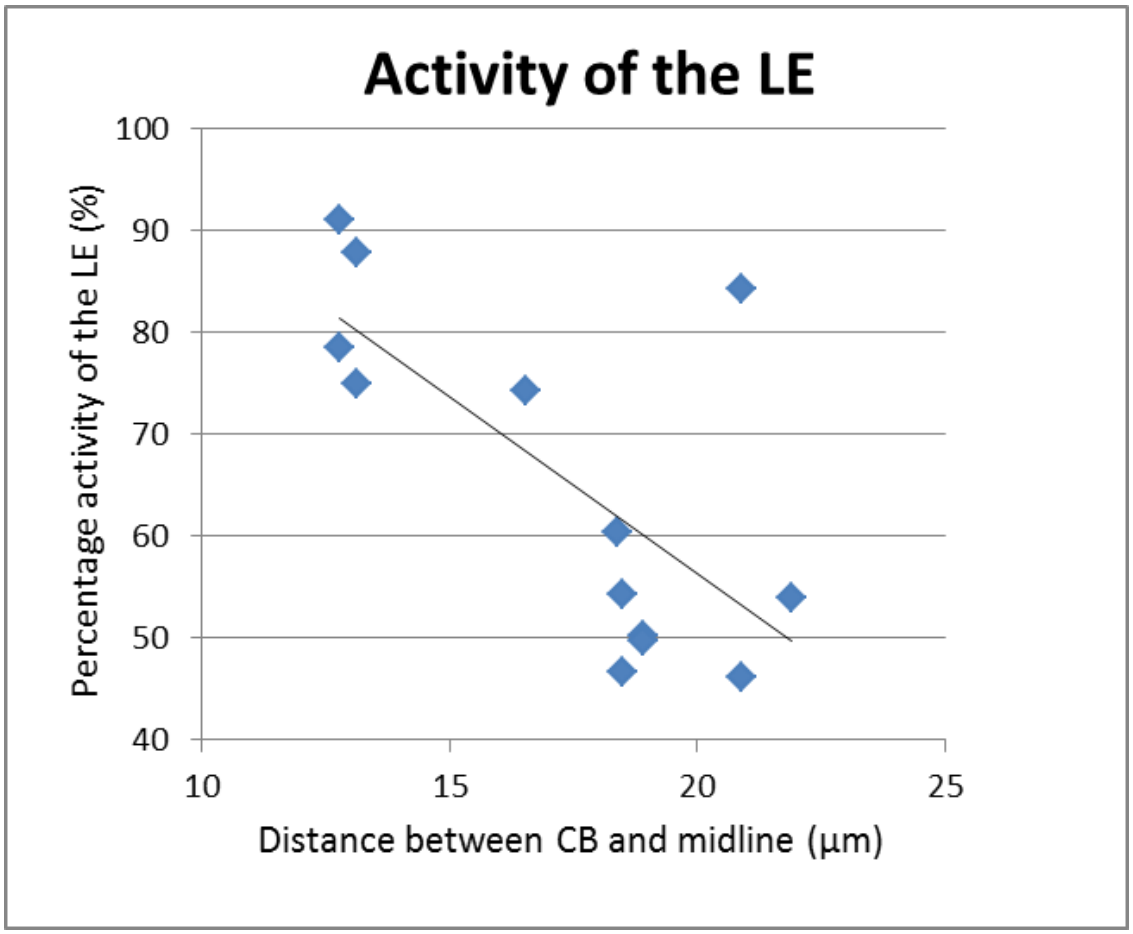
Activity of the LE
Percentage activity of the LE (%)
100
90
80
70
60
50
40
10
15
20
25
Distance between CB and midline (µm)

3.2 Filopodial tips make the first contact between the bilateral rows of cardioblasts

In addition to dorsal view movies, cross sectional movies were also filmed to observe the behaviour of cellular extensions. Previous studies have shown that the CBs initially extend processes dorsally and the first contact between the cells occurs at the dorsal most apical side of the cell (Medioni, et al. 2008). However, it is not known whether filopodia initiate the first contact between the contralateral CBs. Figure 2 shows images taken from time lapse cross sectional movies in live embryos expressing *moesin-mcherry* and *tupGFP*. Moesin localizes to the tips of the filopodial processes (Edwards, et al. 1997) which is consistent in CBs as well (Fig. 6). Once the first contact was made it was maintained throughout the rest of the development (Fig. 6 B,C). After the contact had been made, the morphology of the cells changed from pear shaped into round shaped which took approximately 10 minutes (Fig. 6D). Medioni et al reports that once the dorsal-apical contact is established, ventral processes are then extended (Medioni, et al. 2008). From their results is appears that Robo/Slit repulsion is already present when the ventral processes are extended. Their analysis suggests that even though the luminal domain is repelling away from the midline, the ventral apical domain is still in search of its binding partner. Unfortunately, due to twitching of the embryo and bleaching of the signal it was difficult to image this stage of development. However, we observed that the dorsal attachment of cell spread ventrally until a sufficient length of membrane contact was made and no ventral processes were observed at this point (Fig. 6D). On the contrary,

it might be possible that Robo mediated repulsion is initiated once the whole apical domain of the CB is together.

Figure 6. Cellular extensions initiate the first contact between contralateral partner cells. (A-D) Cross sectional images taken from time lapse movies are shown. (A-B) CBs display migratory behaviour with their pear shaped morphology. Cytoplasmic processes are extended at the dorsal-apical domain of the cell (Arrow). (C-D) Once contact is made between the partner cells, the cells bodies migrate closer to one another and switch their morphology from pear shaped to round shaped. CB nuclei are marked with arrowheads. Pericardial nuclei are marked with asterisks. The images were taken ten minutes apart with a merged Z-stack of 5-7μm.

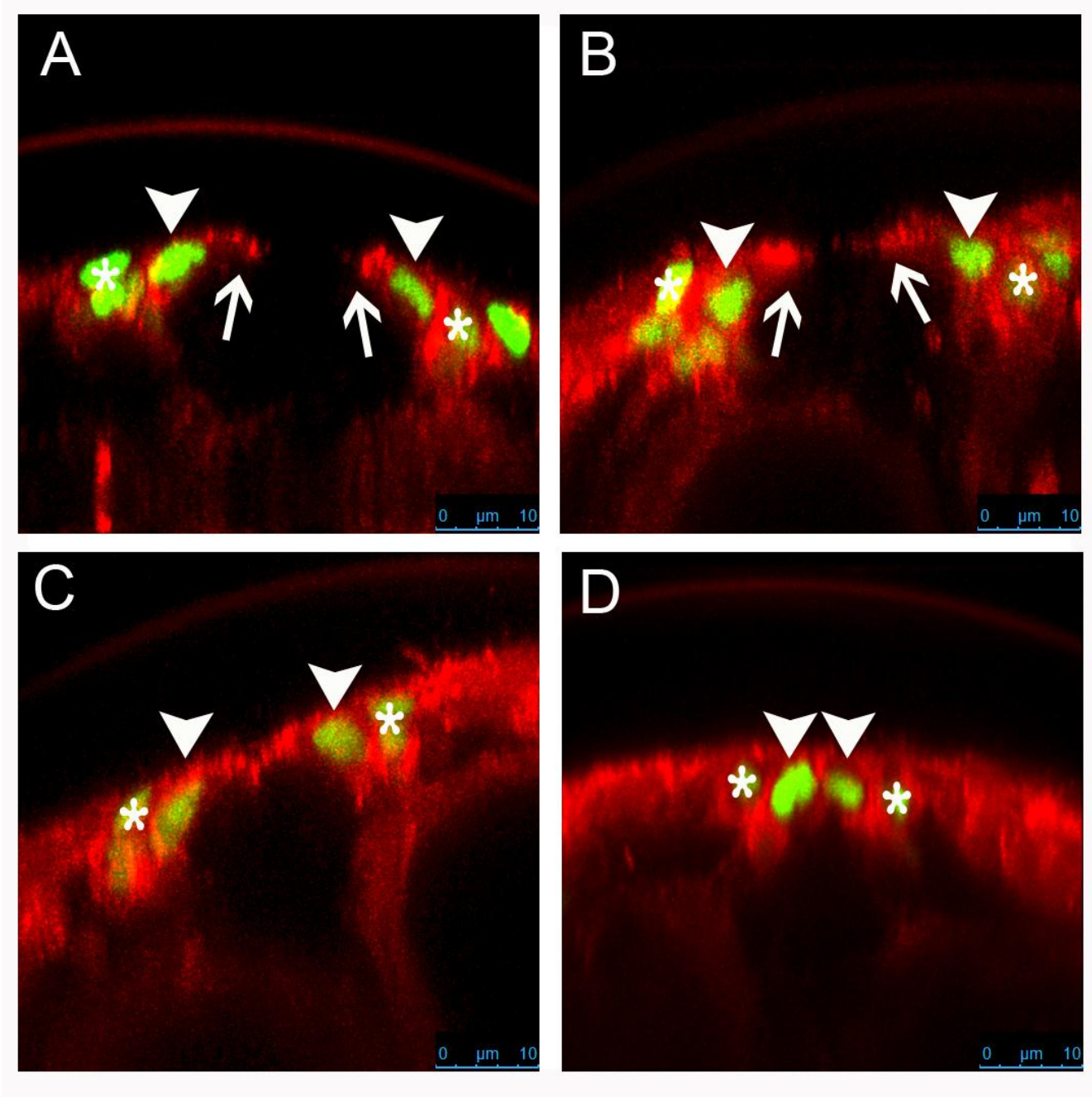
A
0 µm 10
B
0 µm 10
C
0 µm 10
D
0 µm 10

3.3 Cardioblasts physically interact with the internalizing amnioserosal cells and the overlaying ectoderm

Prior to migration, both ectodermal and CB LEs align into bilateral rows on each side of the embryo. After germ band retraction these LEs migrate together towards the dorsal midline. Our analysis of cross sectional EM images of fixed embryos suggested that both these LEs migrate together and interact at later stages of dorsal vessel development (Fig 2E,F). In addition, dorsal closure results in internalization of AS cells into the embryo, particularly the site at which the future dorsal vessel is going to form. Therefore, it was important to study the location of AS cells relative to the CBs before their fusion with contralateral partners to see if any direct interaction is present between these tissues. To observe the behaviour of AS cells we used a ubiquitously driven *DE-cadherin-GFP* construct along with *dmefGAL4* and *UAS-moesin-mcherry*. When we looked at time lapse movies of embryo expressing the constructs mentioned above, we observed that AS cells were marked with *DE-cadherin-GFP* along their apical plasma membrane. As dorsal closure ends prior to dorsal vessel fusion at stage 16, we observed that the distance between the AS and most centrally located CBs along the bilateral row was on average 12 μm (n=6 embryos). The time it took for the CBs to cover the 12 μm distance to the AS cell was approximately 25 minutes (n=6 embryos). As the anterior and posterior part of bilateral rows came closer to the midline we observed an increase in filopodia on the cells surface of the cells which were directed towards the internalizing AS (Fig. 7,8). We observed that the heart cells only approached their contralateral partners once the ectodermal cell fusion had already occurred. This suggested that CBs

located in specific segments are only able to contact the opposite row once the ectoderm has fused and dorsal closure is complete at that individual segment. After the formation of continuous ectoderm AS cells lose contact with the ectoderm and are internalized (Nilufer Mohseni, Reed lab personal communication).

To observe the relative location of AS in respect to ectoderm and CBs, cross-sectional movies of embryos expressing the constructs mentioned above were collected. Because AS cells contain adheren junctions, DE-cadherin is localized to the cell surface of the AS cells at the apical domain. In time lapse movies we also observed that DE-cadherin was localized to the apical domain of the AS cells. Our results illustrate the loss of contact between AS cell and the ectoderm (Fig 7C). CBs extend processes over the internalizing AS cells once they have lost contact with the ectoderm (Fig 7D, arrow). This observation suggests that AS cells that maintained junctional adherence with the Dorsal Most Epidermal (DME) cells, must lose contact with the ectoderm for the heart cells to come in contact. Additionally, we observed that as the CBs extend processes over the apical side of AS cells (Fig 7D, arrow), they also appear to contact the AS cells at the luminal domain (Fig. 7C, arrowheads). However, AS cells when extruding, occupy the space where mature dorsal vessel will be located. This means, even though the dorsal apical side of the CBs have already formed junctions, the AS cells are blocking the interaction between the central and ventral apical region of the CB. From this data it can be concluded that AS cells must fully internalize in order for lumen formation to be completed.

One caveat of using the *ubi-DE-cadherin-GFP* construct is that the ectodermal cells are not labelled well. Also, the chromosome had another insert *ftzGAL4* which was causing problems in assessing LE morphology. Because of this I used another construct to label ectodermal cells in addition to the AS cells. Basigin is an integrin-associated transmembrane glycoprotein which is highly enriched in both developing embryo and extraembryonic tissue such as the AS. A homozygous viable protein trap transposon (PTT) line that reports basigin expression as a basigin-GFP fusion protein was used to label the AS and the ectodermal LE cells (Reed, et al. 2004). The expression of this construct helped in visualization of the ectodermal cell boundaries and AS both in cross sectional and dorsal view movies (Fig 8).

We generated time-lapse movies which encompassed all the stages of heart development using the *bsg-PTT* construct along with *moesin-mcherry* expression in the CB. At stage 15, the distance from the CB LE to the ectodermal LE ranged from 10-20μm (n=6). The distance between the partner CB appeared to be less where ectodermal fusion had already taken place (anterior and posterior of heart) (Fig 8A,B, arrows). In stage 16 embryos, the distance between the CB and ectodermal LE was reduced and on average was 10μm (n=6) (Fig 8C,D). At this stage, the apical membrane of CBs appeared to be restricted by the basal domain of the ectodermal cells (Fig 8C, arrowhead). However, filopodial extensions by CBs were present and our Z-stack analysis of the movies suggested that these processes occupy the space between the ectodermal cells and internalizing AS cells (Fig 8E). This is further shown in cross-sectional movies which demonstrated the localization of AS, ectodermal and cardiac cells relative to one another.

In these movies AS cells were observed to occupy the space at the midline below the ectoderm where the future dorsal vessel is going to be formed (Fig 8E,F). As in previous cross-sectional movies, CB had pear shaped morphology and extended processes dorsally. The contact of CB with the ectodermal and AS cells was observed to be present. In regards to ectodermal cells, their contact with CB was maintained throughout heart development (Fig 8E,F). Based on these observations we concluded that CB interact with both ectodermal and AS cells physically as was shown by EM images of fixed embryos.

Figure 7. Cardioblasts physically interact with amnioserosa cells. (A-D) Images from time lapse movies expressing *ubi-DE-cadherin-GFP*, *dmef::moesin-mcherry* and *ftz::moesin-mcherry* constructs are shown. CB, pericardial cells and AS cells are marked with CB and AS respectively. (A) Dorsal view of embryos at late stages of dorsal closure. CBs extend Filopodial processes which are oriented towards the AS (arrowhead). At this stage AS cells have not yet lost contact with the ectodermal cells and are covering what is left of the dorsal hole. (B) At stage 16, we observe the apical side of the AS cells localized at the middle of the dorsal hole. At the anterior and posterior part of the AS we observe AS cells which are already internalized into the embryo and ectodermal adhesion is completed at those segments. Filopodial processes are observed to interact with the AS cell at this stage (arrowhead). (C,D) Cross sectional views. (C) CBs are located beneath the ectoderm and interact with both the AS cells and ectodermal cells (arrowhead). Cadherin is localized to the apical domain of the internalizing AS cells (GFP). CB processes are extended over the AS cells. (D) At late stages, CBs appear to contact their contralateral partner cells over the AS cell (arrow without label). Contact between the AS cell and CBs in indicated by the arrowhead. (E) Image showing the contact between cardioblast filopodia and AS cells (arrow). Anterior of the heart is to the left on panel A and B. Dorsal side is towards the top in panels C and D. The *ftzGAL4* drove the expression of *moesin-mcherry* in the even numbered segments of the ectoderm. Only the segments where *ftz::moesin-mcherry* expression was absent were used for analysis.

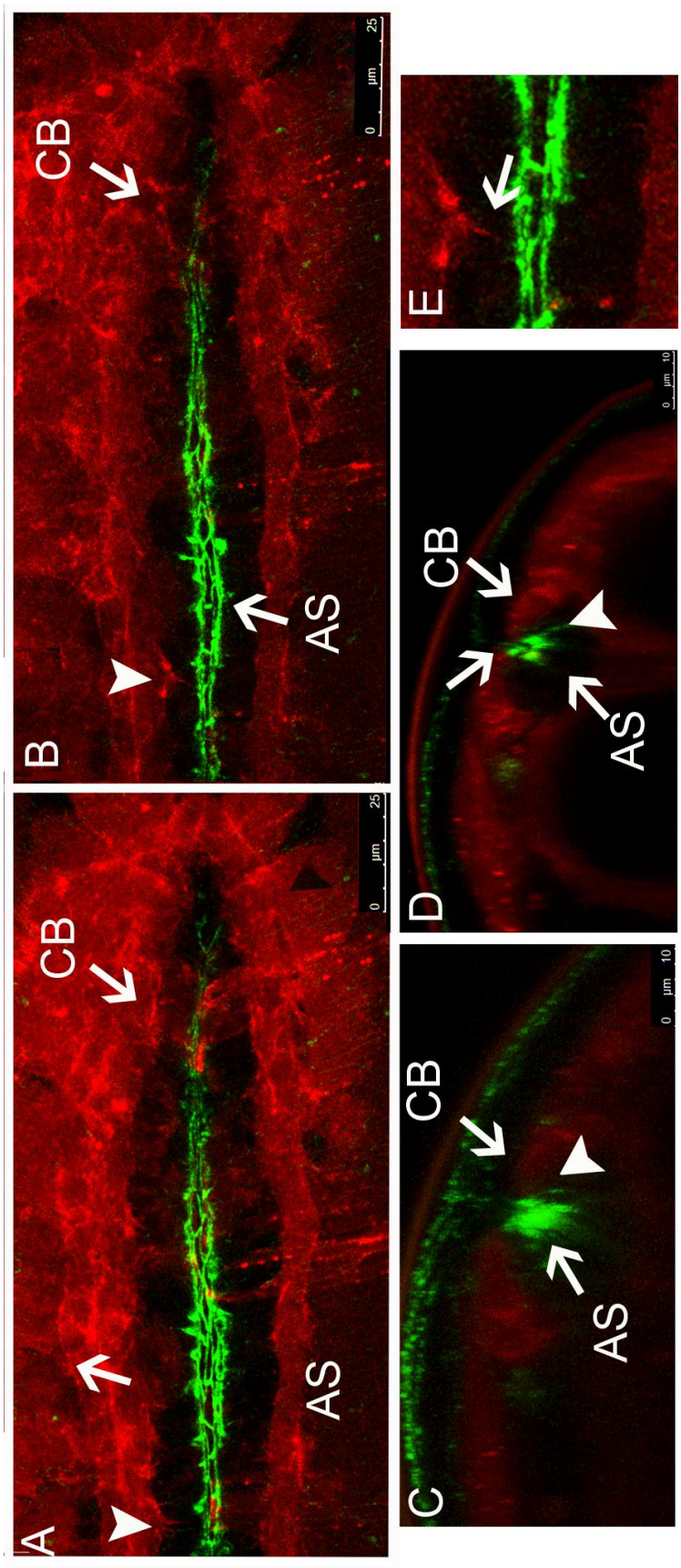
A
CB
AS
0 µm 25
B
CB
AS
0 µm 25
C
CB
AS
0 µm 10
D
CB
AS
0 µm 10
E

Figure 8. Cardioblasts physically interact with ectoderm and amnioserosa cells. A-F) Images were taken from time lapse movies expressing *bsg*-PTT GFP line along with *UAS-moesin-mcherry* under the control of *dmefGAL4*. (A-D) Dorsal view of an embryo undergoing dorsal closure. Ectodermal fusion occurs prior to CB contact (arrow indicates the completion of ectodermal fusion). CBs extend filopodial processes which contact the AS (arrowhead). (B) As the dorsal closure progresses AS is internalized and CB begin contacting the opposite row, initially at the most anterior and posterior area of the LE (arrows). (C) DME cells undergo fusion to cover the dorsal hole as the AS is internalized into the embryo. Cardiac cells stay behind the most dorsal ectodermal cells. It also appears that the basal membrane of the ectodermal LE cells restricts the CB migration (arrowhead), however filopodia are extended by the CB LE which contact the AS cells (arrow). (D) As the AS is further internalized, bilateral rows start to fuse starting from the peripheral cells of the LE towards the central cells. (E-F) Cross sectional images were taken from time-lapse movies. AS cells are internalized between the CB bilateral rows. CBs extend processes over the AS cells. CB and AS cells are marked with arrows. Contact between AS and CB is marked with arrowheads. Anterior of the heart is towards the right hand side in panel A,B,C and D. Dorsal side is oriented towards the top in panel E and F. (G) High magnification image showing the protrusive behaviour of filopodia. CB extend filopodial processes into the space between the AS cells and DME cells. EC refers to the LE cells of the ectoderm (arrows, arrowhead).

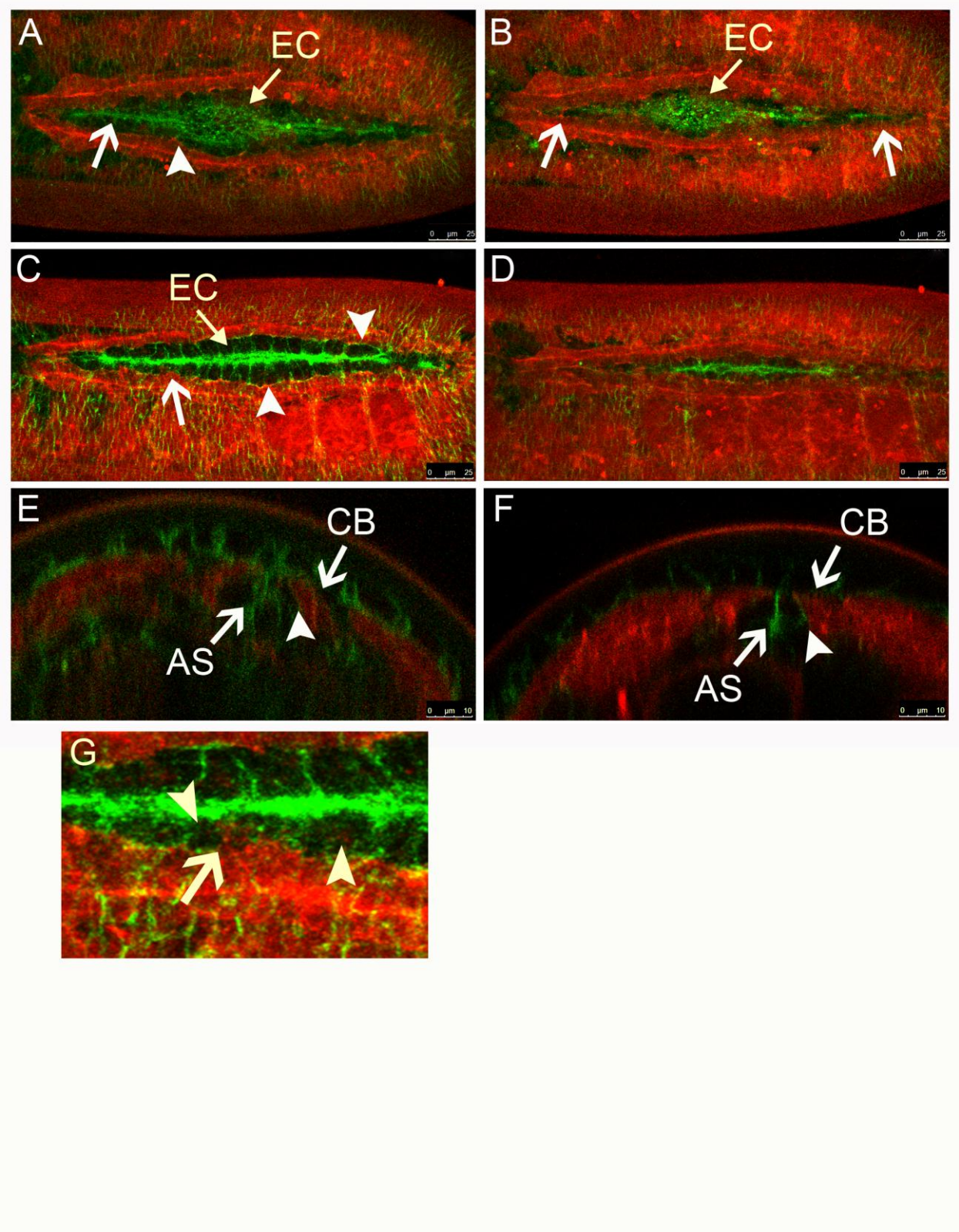
A
EC
B
EC
C
EC
D
E
CB
AS
F
CB
AS
G

3.4 Kuzbnanian plays a role in cardioblast migration

ADAM metalloproteases such as *kuzbanian* are required for proteolytic cleavage of membrane bound proteins (Rooke, et al. 1996; Lieber, et al. 2002). Initially Kuzbanian was identified as a protease which is responsible for cleavage of Notch receptor (Lieber, et al. 2002). The role of *kuz* in *Drosophila* was determined to be the cleavage of Notch receptors upon its activation. Notch is required for lateral inhibition of CBs and therefore it has been reported that when *kuz* is absent, a hyperplastic heart is formed which has approximately double the number of CBs compared to wild-type heart (Albrecht, et al. 2006). Additionally *kuz* is required for axon guidance during CNS development (Coleman, et al. 2010). Along with Robo/Slit, *kuz* is required for formation of the proper ladder like structure of axons. Since it is known that *kuz* cleaves Robo receptor to promote Robo signalling (Coleman, et al. 2010), and Robo is required for generation of cellular extension in CBs, I wanted to study whether *kuz* also plays a role in generation of cellular extensions.

We expressed a dominant negative version of Kuz and observed its effect on the LE morphology. Since the GAL4-UAS driver is temperature sensitive system, we produced time lapse movies of embryos incubated at varying temperatures. Since the GAL4-UAS systems is optimally induced at 29˚C and minimally induced at 18˚C, *kuzDN* expression would vary if incubation temperatures are fluctuated. As a control we incubated embryos first at 18˚C, or 25˚C and then performed an experimental temperature shift where initially embryos were incubated at 18˚C until they reach stage 13 and then at 29˚C till filming. This was done to ensure that the expression of KuzDN contruct

interferes less effectively with the lateral inhibition and so no hyperplastic heart is formed. However, in time lapse movies of embryos incubated at 18˚C we observed some duplication of CBs (Fig 9 B', arrow). Since at 18˚C the GAL4-UAS system is not optimally induced, less duplication of the cells took place compared to 25˚C embryos due to insufficient expression of kuzDN. Integrity of the LE was maintained in most of the segments. However, a gap spanning two cell diameters was observed at the heart region of the dorsal vessel (3/5 embryos) (Fig 9 B-B'', arrowhead). Migration speed of CBs was also affected and was measured to be 0.31μm/min (Table 2). Next, embryos staged at room temperature were filmed. Major duplication of CBs was observed which suggested absence of Notch based lateral inhibition due to expression of KuzDN construct at earlier stages of development (Fig 9, C-C'', arrows). Interestingly, the anterior part of the aorta region travelled to the midline faster compared to the heart region and posterior part of the aorta region. This phenotype was also noticed in the 18˚C embryos where the anterior part of the heart made first contact with the bilateral row before the posterior region.

Finally, we looked at embryo which were grown to stage 13 in 18˚C and then switched to 29˚C until stage 15 to induce the maximal expression of the *kuzDN* construct. The number of CBs present in these embryos was comparatively similar to the 18˚C incubated embryo (n=5). Some duplication of the CB took place, however a hyperplastic phenotype was weak (Fig 9D''). This suggested that Notch based lateral inhibition took place while the GAL4-UAS system was less active. Filopodial activity in these embryos was not affected and the migration speed appeared to be normal at 0.38 μm/min (Table 2). The percentage LE activity at stage 15 was 40% and increased to 65% at stage 16, which

indicates wild-type behaviour of the LE. Together, the data suggests that *kuz* does not play a role in Filopodial extension.

Figure 9. Heart development in KuzDN mutants. Images were taken from time lapse movies expressing *moesin*-mcherry and *kuzbanianDN* under the *dmefGAL4* driver along with *tupGFP* staged at various temperatures. (A-A") In wild-type embryos without *kuzDN expression,* CBs migrate towards the midline with highly active LEs and fuse together.(25˚C) (B-B") In embryos staged at 18˚C, mild duplication of cells was observed (arrows). The anterior part of the LE reached the midline faster than the posterior heart region. A gap spanning two cell diameter was present at the heart region of the dorsal vessel (arrowhead). Filopodial activity appeared to be normal. (C-C") In embryos staged at 25˚C, duplication of cells was observed in all segments of the heart (arrow). Migration was delayed in these embryos; however the Filopodial activity appeared to be normal. (D-D") In embryos which were shifted from 18˚C to 29˚C at stage 13, we observed some duplication of cells which resembled embryos from the 18˚C control experiment. The cells were able to extend Filopodial processes which were abundant through the entire LE.

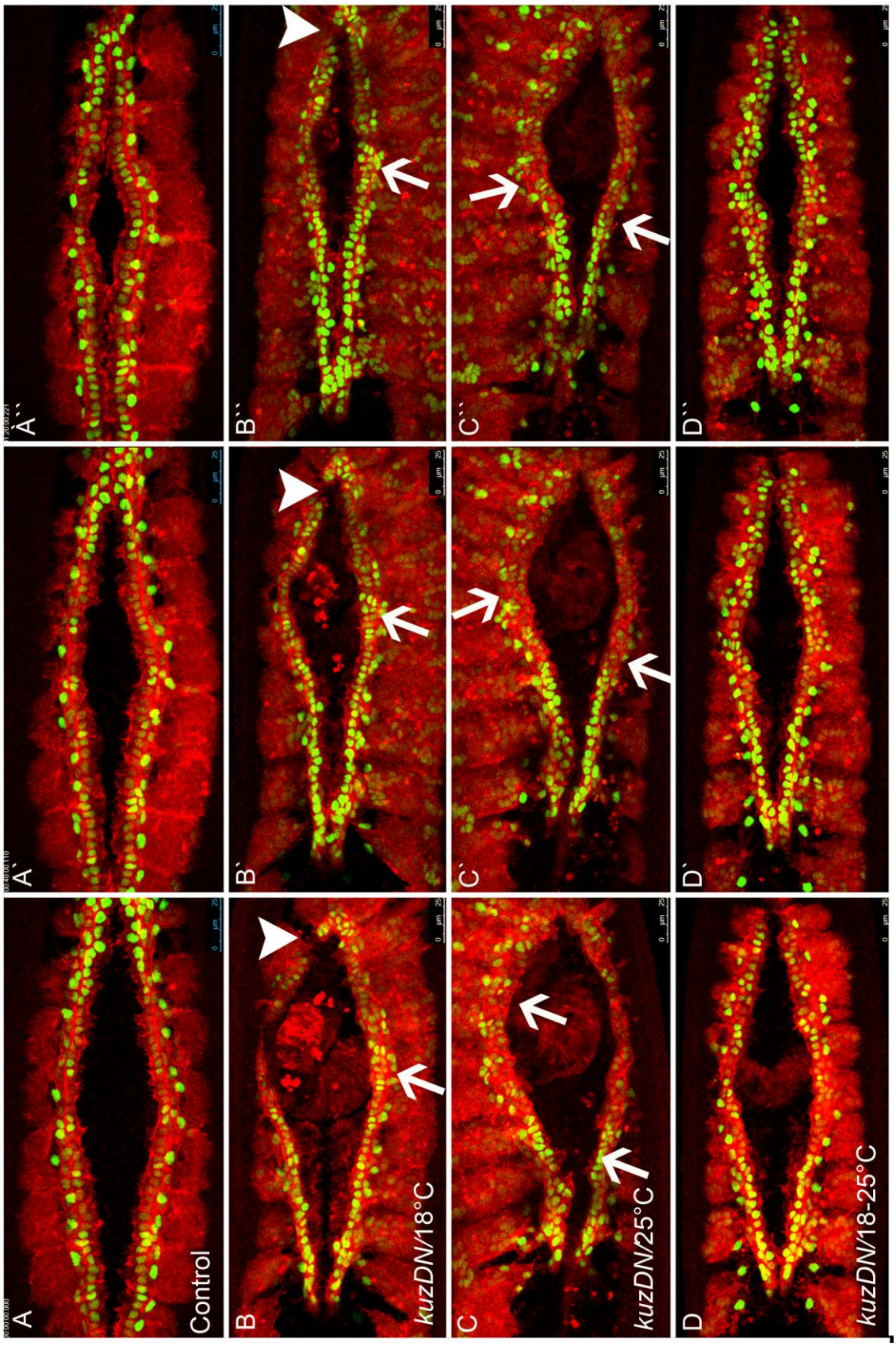
A
Control
B
kuzDN/18°C
C
kuzDN/25°C
D
kuzDN/18-25°C
A`
B`
C`
D`
A``
B``
C``
D``

Table 1. Percentage activity of the Leading edge in several backgrounds. Activity of the LE is represented as a percentage in the table below. Movies of wild-type, *slit*, *robo* and *leak* mutants, *robo* RNAi and *kuzDN* embryos were used for the calculation. Measurement of filopodial activity for stage 15 and stage 16 is shown separately. For each measurement an average of 10 LEs were used, except *robo,leak* RNAi for which 6 LE were used in calculations. “n” refers to the number of LEs used for measurement.

Table 1. Percentage activity of the leading edge in different backgrounds

Background	Percentage Activity of LE (Stage 15)	Percentage Activity of LE (Stage 16)
Wild-type (n=13)	46%	73%
slit mutant (n=10)	19%	32%
robo, leak mutant (n=10)	19%	40%
Robo, leak RNAi (n=6)	23%	34%
dmefGAL4xKuzDN (temperature shift) (n=6)	40%	65%

3.5 Robo plays a role in extension of filopodia

Robo and its ligand Slit are required for lumen formation in dorsal vessel. Studies and findings from our and other labs suggest that Robo/Slit might play a role in CB migration and overall cardiac morphogenesis (Qian, et al. 2005; MacMullin and Jacobs, 2006). Additionally it has been shown that Robo inhibits filopodial exploration at the neuropile (Murray and Whitington, 1999). This led us to ask the question does Robo plays a role in filopodial extension of the LE? To answer this question we down regulated *robo* levels by expressing double stranded RNA constructs of *robo* for each Robo gene expressed (Robo1, Robo 2 and Robo3) in the CB using the *dmefGAL4* driver. *Moesin-mcherry* and *tupGFP* were used as markers to visualize the CB LE and nucleus respectively.

In *robo* RNAi mediated knockdown embryos, formation of continuous bilateral row was normal. CBs were successful in reaching the midline and fusion between appropriate contralateral partners occurred. The migration speed of the CB was heavily affected and took 90 minutes to proceed from stage 15 to late stage 16 (0.18μm/min), which in wild-type embryos requires 45 minutes (0.38μm/min) (Table 2). At stage 15, some filopodial activity was observed at the posterior and anterior part of the heart (Fig 10 B-B'', arrow); however the central region failed to extend filopodia. In wild-type embryos by late stage 16, the LE is almost completely active (Table 1) (Fig 10 A-A''). In *robo* down regulated embryos the LE activity increased from 23% (Stage 15) to 34% (Stage 16) (Table 1). Since filopodial activity was lower in these embryos we came to the conclusion that Robo might play a role in Filopodial extension by regulating cytoskeletal

rearrangement. Nevertheless, we observed some basal level of Filopodial activity present. This might be due to partial depletion of Robo by the dsRNA.

Hence, we looked at LE in *robo1,leak* double mutants. Apart from the presence of gaps (not shown) and delayed migration, we observed a less active LE compared to the wild-type (Table 1). At stage 15, 19 % of LE was active and by late stage 16 LE activity increased to 33.6%, which compared to wild-type is much lower (Table 1). Delayed migration was observed in some cases where the entire or part of the LE did not migrate along with the rest of the bilateral row. This observation indicates that Robo might play a role in regulating cytoplasmic extension directly or indirectly.

Figure 10. Filopodial activity of cardioblasts in *robo* mutant embryos. (A-A’’’) Images from time-lapse movies of wild-type embryos were collected and are shown below. Images are ten minutes apart. Filopodia are present all along the LE (arrow). (B-B’’’) Images from time-lapse movies of embryos in which *robo* levels were knockdown using RNAi are shown. Images shown below are 20 minutes apart from one another. Filopodial activity appears to be lower than wild-type, however some filopodial activity is present (arrow). As the development progresses, filopodial activity does not increase in the CB. (C-C’’’) Images from time-lapse movies of *robo* and *leak* double mutants are shown below. Images are 15 minutes apart. Delayed migration is observed (arrow). Filopodial activity is present however appears to be less compared to wild-type (arrowhead). Anterior of the heart is to the right.

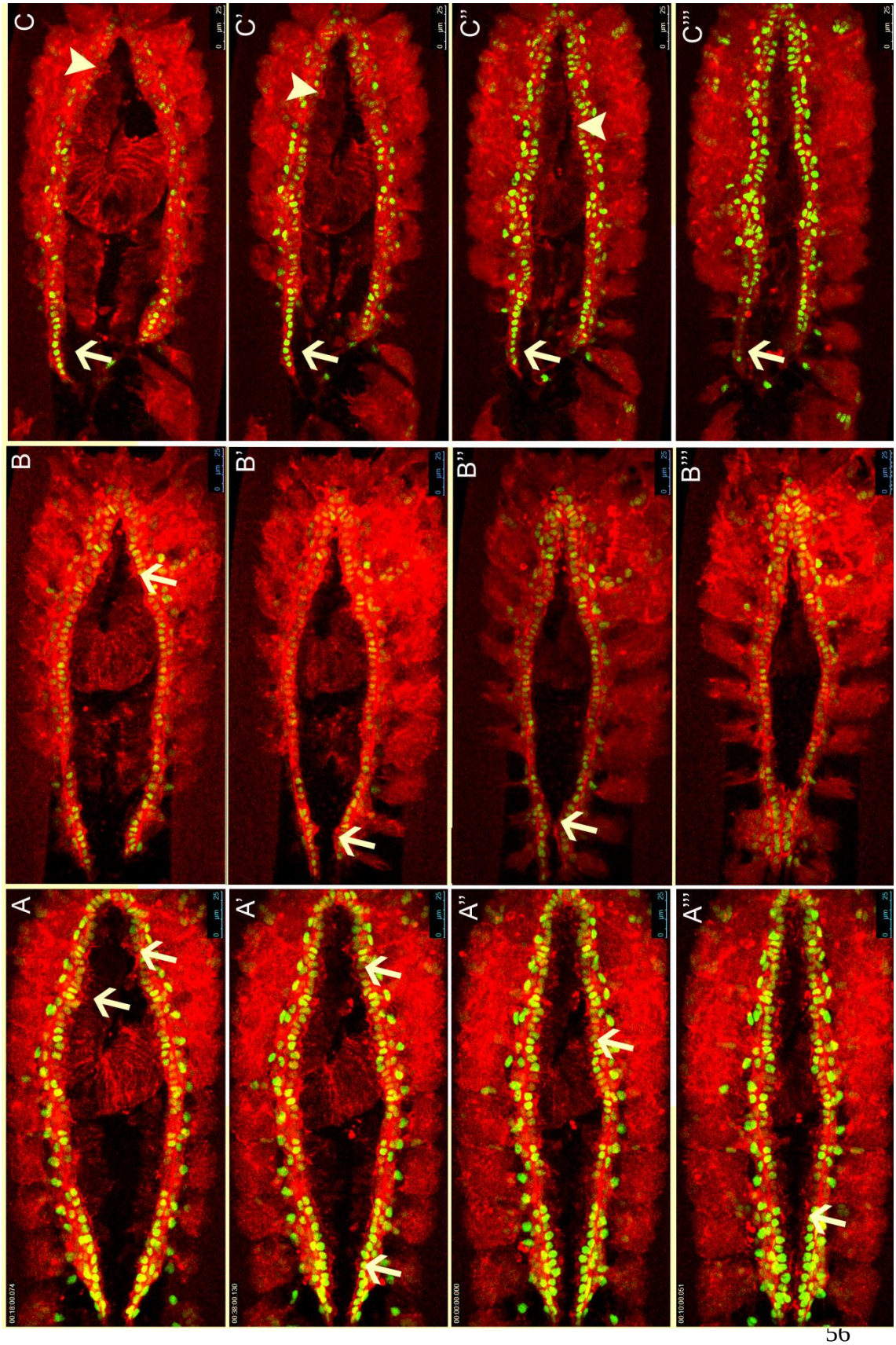
A
A'
A''
A'''
B
B'
B''
B'''
C
C'
C''
C'''

3.6 Slit down regulation affects heart development and filopodial extension

Previous studies have reported that Slit is required for dorsal vessel formation, particularly lumen formation, maintenance of LE integrity, CB migration and cell polarity (Qian, et al. 2005; MacMullin and Jacobs, 2006; Helenius and Beitel, 2008). Since we discovered that Robo plays a role in Filopodial extension and CB migration, it was imperative to observe the effects of *slit* RNAi mediated knockdown on CB. We performed a tissue-specific down regulation of Slit using a ds RNA (RNAi) construct against *slit* in the CB using a *dmefGAL4* driver. To confirm that the expression of RNAi resulted in reduction of Slit, antibody labelling of Slit was performed in embryo where Slit was down regulated in only *svp* expressing cell (Dutchak K., supplementary data). Normally, Slit localizes to the apical side of the CB during late stages of heart development. We observe this localization to be absent at the apical side of *svp* expressing cells (+/+; *svpGAL4/UAS-slit-RNAi)*. Normal localization of Slit was observed in *tinman* expressing cells where Slit dsRNA was not expressed. This demonstrated that Slit dsRNA expression results in down regulation of Slit.

We used *UAS-moesin-mcherry* construct along with *dmefGAL4* to visualize the LE of the CB. We observed no apparent decrease in activity of the LE in Slit RNAi mediated knockdown embryos where the percentage activity of LE was 39% at stage 15 and 70% at stage 16 (Table 1). CBs were able to migrate to the midline without any visible defects. However, gaps spanning one or two cell diameters were observed in such embryos (2/6) (Supplementary material Fig 14). These gaps were identified by the absence of apical

membrane since the nuclear marker , *tupGFP* was absent from these embryos. Furthermore, ipsilateral cells adjacent to the gaps were able to extend filopodia into the gap and contact the opposing cell (Supplementary material, Fig 14). This is interesting since filopodia are only expected to be extended by the apical side and not the lateral side of the cells. These contacts were short lived which indicated that contacts are only stabilized once the contact between contralateral partners is achieved. In addition, the contralateral partners of the missing cells were able to migrate to the midline and extended Filopodial processes into the gap (Supplementary material, Fig 14). Contact between these cells was made with the cells neighbouring the gap, however, once again no contact stabilization was observed.

Even though we demonstrated that *slit* expression level reduction occurs in cells expressing dsRNA against Slit, our data was not consistent, with only 2/6 embryos showing a phenotype. This might be due to partial down regulation of Slit. To account for the inconsistency we decided to observe filopodial behaviour in *slit* loss of function mutants. Time-lapse movies of *slit* homozygous mutants were filmed, in which nuclei of CBs and filopodia were marked by *tupGFP* and *moesin-mcherry*, respectively. Gaps spanning several cell diameters were seen in all mutant embryos (Fig 11 B-B’’’, arrowheads). Cell clumping was also observed in several cases (Fig 11B, arrow). Filopodial activity of the LE also appeared to be lower than wild-type, however, some basal activity was still present. In wild-type embryos, it is expected that the anterior and posterior part of the CB LE extends the processes first. It is also expected that once the CB are near the midline, the filopodial activity increases significantly throughout the LE.

In *slit* mutants, filopodial activity was reduced at all stages of heart development (Fig 11 B-B’’’, arrow). At stage 15 19% of LE was active and by late stage 16 it was 34%.[n=8] (Table 1). Cell migration speed was also measured in these embryos which was 0.23 μm/min (Table 2). Since slit mutant LE activity and migration speed is significantly lower the wild-type LE activity (Table 1,2), Robo signalling via Slit might be required for filopodial extension of CBs.

Figure 11. Filopodial behaviour in *slit* mutant embryos. (A-A’’’) Wild-type heart development is shown at different stages of development. CBs extend filopodial processes all along the LE. (B-B’’’) Several gaps in the LE are observed to be present (arrows). Small cluster of cells are also present along the bilateral rows (arrowheads). The activity of filopodia is decreased compared to wild-type in these embryos. CB cell shape appears to be circular rather than pear shaped as in wild-type. Anterior is towards the left.

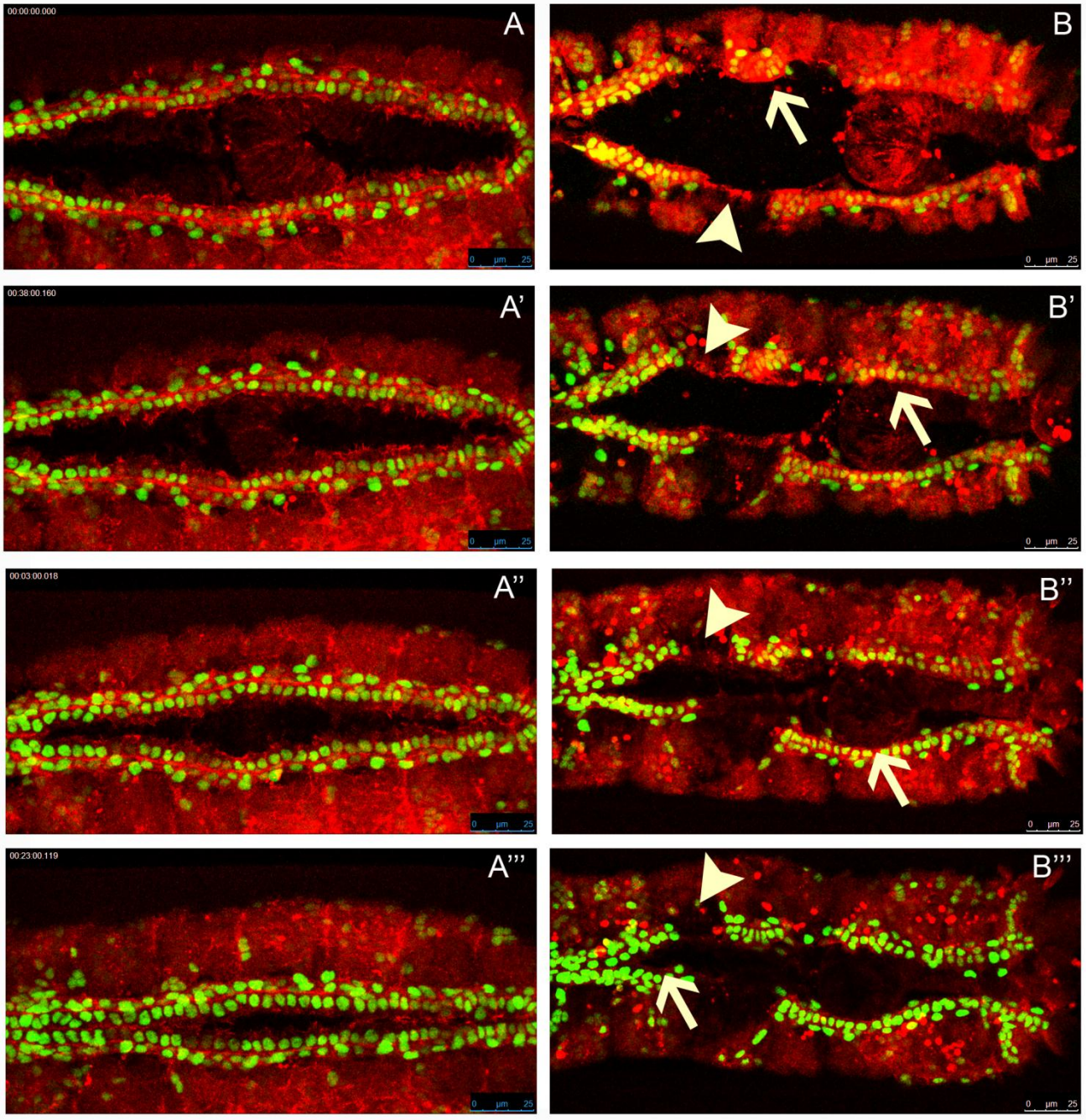
00:00:00.000
A
B
0 µm 25
00:38:00.160
A'
B'
00:03:00.018
A''
B''
00:23:00.119
A'''
B'''

Table 2. Cardioblast migration speed. Cell migration speed was measured as described in the Material and Methods section for each genotype mentioned in the table. All the embryos expressed *tupGFP* nuclear tag and *moesin-mcherry* tag. The number of embryos (5 cell pairs from each embryos) for which the migration was calculated are indicated as "n". The speed is presented in μm per minute. In *kuzDN* experiment, embryos which were grown in temperature shift were used for calculations.

Table 2. Migration speed of CB in different genetic backgrounds.

Background	Cell migration speed (μm/min)	Standard Deviation (±)
Wild-type (n=12)	0.38	0.047
slit mutant (n=8)	0.23	0.055
robo, leak mutant (n=8)	0.25	0.096
Robo, leak RNAi (n=3)	0.18	0.064
dmefGAL4xKuzDN (n=5)	0.31	0.055

CHAPTER 4: Discussion

4.1 Cardioblasts extend filopodial processes which may participate in the recognition process of contralateral partner cells

Extension of filopodial processes is a basic feature that is present in most migrating cells. One of the examples is the migrating ectodermal cells which cover the AS to form a continuous ectoderm. These cells are capable of extending long filopodial processes which have been well characterized by Thomas Millard and colleagues (Millard and Martin. 2008). They showed that before zippering of the ectoderm, filopodia of the ectodermal LE contact their partner cells. In this case, there are several different subtypes of cells along the ectodermal LE, two of which are the *patched* expressing cells and *engrailed* expressing cells. Localization of these cells is very precise and each segment of the embryo at the LE contains both cells. For the proper zippering of the ectoderm and to maintain registration of segmental boundaries, it is crucial that the filopodia from the matching cells contact one another and once the recognition has occurred, form tethers and fuse together. It was shown that only filopodia extruded from matching cells were able to form stable contact. However, when mismatching cells contacted one another no stable contact was made and fusion did not occur (Fig 4). This experiment demonstrated that filopodia are able to distinguish between partner and non-partner cells.

We speculated that these filopodial processes are also extended by the migrating CB which migrate behind the ectodermal cells. Therefore, our first objective was to check for the presence of the filopodia in the CB LE. Using the *UAS-moesin-mcherry* construct

we were able to visualize the filopodia of the CB LE. This confirmed that CB, like the ectodermal LE, was able to extend filopodial processes towards the direction of migration. Our high magnification images of live embryos suggested that filopodia were able to extend and retract extensively and there were more than one filopodial extension per cell.

We demonstrated that CB LE, like other migrating cells, is capable of extending filopodial processes which resemble filopodia of the ectodermal LE (Millard and Martin. 2008). What is yet unknown are what role these processes play in heart development. This brings us to our next objective, which was to assess the specificity of contact of the CB filopodia in regards to contralateral, non-contralateral and ipsilateral cells. This experiment was done to study the recognition mode of filopodia once they contact other cells. We showed that filopodial processes interact with contralateral and non-contralateral cells equally when they are within contact distance (Fig 3). The formation of stable contact however was only observed once the contralateral partner cells contacted one another. This stable contact was not observed to be present in cells which contacted non-partner cell (Fig 4). This shows that filopodia discriminate against non-contralateral cells when it comes to adhesion formation. Since this observation is also present in ectodermal LE, it might be possible that same matching mechanism exists in CB as well. Since the CB LE contains two different kind of cells, *svp* and *tinman* expressing cells, it might be possible that the precise adhesion of cells requires *svp* and *tinman* expressing cells to form adhesions with their identical partners on the opposite row. In this model, filopodia from *svp* expressing cells only form stable contact with filopodia from opposing

svp expressing cells. Subsequently, *tinman* cells will also exclusively form adhseions with *tinman* cells on the opposing row.

Furthermore, down regulation of genes such as *slit, de-cadherin,* and *robo,* results in loss of CBs from the bilateral rows (Santiago-Martinez, et al. 2008). This study also reports the presence of gaps in these mutant embryos which spanned from 2-6 cell diameters. In this case, when a neighbouring cell was absent it was observed that these cells were able to extend filopodial processes into the gap from the lateral sides of the cells (supplementary material, Fig 14). In embryos where gaps of two cell diameter were observed interaction between the ipsilateral cells was observed which were spanning the gaps. This contact was very brief and did not result in tethering of the filopodia.

Finally, we report that CB LE is highly active and extends filopodial processes. The extension of the filopodia are present at specific section along the LE. Furthermore, filopodia appear to be specific in recognizing their contralateral partner cells. In muscle synapse formation, proteins have been identified that are required for the recognition processes between axons and muscle fibers (Kohsaka and Nose. 2009). It might be possible that such molecules are also present in CB filopodia which assist in recognition of target cell.

4.2 Internalizing amnioserosa stands in the way of contralateral cardioblasts

During Dorsal Closure the ectodermal LE envelops the AS and fuses together to form a continuous ectoderm at the dorsal side of the embryo. Internalization of the AS cells occurs at the midline where future dorsal vessel is going to be localized. Our results demonstrate that at late stages, when the distance between the internalizing AS cell and

CB is short, CBs extend cellular processes at the dorsal side. Initially it was thought once the CBs are near the midline, they are able to sense their contralateral partners and hence extend filopodial processes in anticipation. In addition, these cellular processes were observed to be oriented specifically towards the midline (Fig 7,8), where the contralateral partners will form the dorsal vessel. However, our cross-sectional images of embryos showed that AS internalization blocks the access of contralateral CBs to one another. The extension of dorsal apical processes by the CB also indicated that, contact between contralateral CB can only occur once the contact between the AS and ectoderm is lost. This observation indicated that CBs are unable to sense their partners because of the internalization of AS which occurs at the midline and blocks their access. Therefore, the extension of processes oriented towards the midline suggested that they are not oriented towards the contralateral partners, but rather the AS cells.

Interestingly, studies have suggested that apoptotic cells are capable of spatiotemporally releasing signalling molecules which affect the surrounding microenvironment (Poelmann and Gittenberger-de Groot, 2005). In the cardiac development of chick, presence of TGF-β signalling molecule was observed to be consistent with the localization of apoptotic cells. This signalling results in myocardialization which requires activation of TGF- β signalling. This result suggests that it might be possible that extracellular matrix surrounding AS releases molecules when undergoing these cells are undergoing apoptosis and promotes signalling in the CBs. In support of this model, we observe that as the bilateral rows migrate closer to the midline the filopodial activity increases significantly. Also, since the most posterior and

most anterior cells are the first to reach midline (closer to the AS cells), filopodial activity on their cell surface increases and this increase is absent from the centrally located CBs (further from the AS cells). Therefore, it might be true that the extracellular matrix surrounding apoptotic AS cells releases signalling molecules which promote filopodial activity of the CB LE.

4.2.1 Contact between amnioserosa cells and CBs might be required to specify the luminal domain

Studies have shown that Robo localizes to the apical membrane of CB during late stages of heart development (Qian, et al. 2005). This localization is required for the proper lumen formation (Santiago-Martinez, et al. 2006). But what localizes Robo to the apical domain? Our initial analysis of cross-sectional images of fixed embryos suggested that CB interact with the internalizing AS cells at late stages of heart development. Interestingly, this interaction is observed to occur at the same time when Robo apicalization takes place (Santiago-Martinez, et al. 2006). Therefore, we suspected that contact dependent localization of Robo is taking place at the apical side of the CB, specifically the luminal domain which interacts with the AS cells. Since the tissue was fixed, we wanted to observe the same stage of heart development in live embryos. Expression of two different GFP constructs (*ubi-DE-Cadherin-GFP* and *basigin-PTT*) helped us label the AS cells and *moesin-mcherry* lit up the CB LE. In live embryos the contact was also observed to occur at late stages (Fig 7). The CBs extended processes over the AS leaving the rest of the apical side in contact with the AS cells. This contact was present all along the apical side which included the luminal domain as well.

Therefore, it might be possible that AS cells instruct the localization of Robo to the luminal domain. Additionally, integrins have been implicated in localizing Robo to the apical side of the side. In *scab* (αPS3 subunit) mutant embryos, Robo and Slit fail to localize at the apical domain. Perhaps, integrin mediated contact between AS cells and CB is required for proper localization of Robo.

4.3 Slit and Robo signalling are required for filopodial extension

Filopodial activity is mostly observed on the leading side of the migrating cells. We showed that the CBs just as any other migrating cells are capable of extending filopodia which are abundantly present on the apical side of the cell. Since filopodia are observed to be highly active, it means that cytoskeletal rearrangement is occurring at high rates on the apical side of the cell. Therefore we would expect this rearrangement to be reduced at the trailing edge. Our data demonstrates that filopodial activity increases at later stages of heart development. Concurrently, at late stages, localization of Robo and Slit also shifts strictly to the apical side where the protrusions are present. This prompted us to ask the question, Does Robo signalling play a role in filopodial activity of the LE? One study showed that Robo decreases branching of the throughout the neuropile which in turn leads to repulsion of the axon growth cone (Murray and Whitington. 1999). This prevents axonal crossing during CNS development. We therefore speculated that Robo might also play a role in filopodial extension in the CB LE. We performed down regulation of both *slit* and *robo* in the CB by expressing dsRNA constructs that would promote degradation of their mRNAs. When we performed RNAi mediated *robo* knockdown, we observed that the activity of the LE was measured to be 23% compared to

wild-type which was 46% at stage 16. A slight increase in activity was observed at stage 16 which was measured to be 34%, whereas the wild-type acitivity was 73%. We also looked at activity in *robo* (*robo1*), *leak* (*robo2*) double null mutants since RNAi mediated knockdown of *robo* may not deplete Robo levels completely. Activity in these mutants was observed to be 19% at stage 15 and 40% at stage 16 (Table 1). This indicated that absence of Robo results in lower filopodial activity at the LE.

Interestingly, a study conducted by Dimitrova and colleges showed that loss of Robo and Slit leads to less branched dendrites (Dimitrova, et al. 2008). Generally, new branch formation involves activation of cytoskeletal rearrangement through actin remodelling. One of the molecules that regulate actin remodelling is Ena, which has been shown to bind to Robo directly and mediate its repulsive signalling in the CNS (Bashaw, et al. 2000). Therefore, it might be possible that Robo indirectly increases the branching of the dendrites. The branching of dendrites requires extension of cytoplasmic processes outwards which is absent in *robo* mutants. Our study also indicates that when Robo is lost, cytoplasmic extensions are also decreased in the CBs. Perhaps rearrangement of the cytoskeleton requires Robo mediated signalling which when absent results in reduced cytoplasmic extensions of cells.

To confirm Slit signalling through Robo is involved in filopodial extension, we additionally looked at LE in the absence of *slit*. In *slit* RNAi embryos we did not observe reduction of filopodial processes. This may be due to the insufficient knockdown via RNAi expression. To account for this, we observed the CB LE activity in *slit* null mutants. Along with several gaps and delayed migration (Table 2) we also observed less

filopodial activity at the LE. The activity resembled *robo* mutants with only 19% of the LE active at stage 15 which increased to 32% at stage 16. Since this phenotype resembled *robo* mutant phenotype, we concluded that Slit signalling via Robo is required for proper extension of filopodial processes in CBs.

4.4 Kuzbanian may be required for late heart development

Kuzbanian is an ADAM metalloprotease which is shown to promote Notch based lateral inhibition during early heart development. It does so by cleaving the intracellular domain of Notch receptor which then serves as a transcription factor and relays signal to the cell. Since it was shown that when *kuz* expression levels are reduced a hyperplastic heart is formed in which the numbers of heart precursor cells are doubled (Albrecht, et al. 2006). This phenotype is due to the absence of lateral inhibition at early stages of heart development. Also *kuz* has been shown to be involved in axon guidance in the CNS (Coleman, et al. 2010). Midline crossing of ipsilateral axons took place when a dominant negative construct of *kuz* was expressed in these cells. Since this phenotype resembled *robo* mutant phenotype, it was proposed that Kuz plays a role in Robo signalling, specifically cleavage of the Robo receptor upon its activation by Slit (Coleman, et al. 2010). Since Robo signalling plays a crucial role in heart development as well, it was interesting to see if Kuz also plays a role in late heart development beside lateral inhibition.

We expressed a dominant negative construct of *kuz* in heart cells at 18˚C, 25˚C and 18˚C-29˚C shift. Our results indicated that at 18˚C, the hyperplastic phenotype of the heart was not present. This was due to partial expression of KuzDN construct because

GAL4-UAS system is not optimally induced at this temperature. However, when embryos were incubated at 25˚C severe hyperplasticity of the heart was observed. Both of these experiments served as controls as the expected phenotypes were present. Next, we observed embryos which were subjected to a temperature shift (18˚C-29˚C). The hyperplastic phenotype was not observed, however duplication of cells was present at several location along the LE (Fig 9). No major disruption of LE integrity was observed which initially indicated that heart cells are able to migrate and fuse with their contralateral partners in the absence of Kuz. The migration of bilateral rows was severely delayed in embryos raised at 25˚C. This might be explained by the presence of excess cells along the LE which might have slowed down the overall migration of the LE. However, in control embryos (18˚C) this delayed migration was not observed. Similar observations were made in embryos in which *robo* was down regulated or absent. Other than cell migration, these results indicate that *kuz* might not play a role in Robo signalling in the heart.

Our results indicate that *robo* RNAi mediated knockdown (and mutant) effects filopodial activity of the LE (Fig 10). Since Robo and Kuz are shown to interact genetically and both are involved in midline repulsion of axons in the CNS, I predicted that *kuz* down regulation might affect filopodial extension by the CB as well. When we looked at all movies in which KuzDN construct was expressed, we did not observe any loss of filopodial activity. In fact, presence of filopodial activity in KuzDN embryos resembled wild-type activity (Fig 9). Therefore, we conclude that Kuz is not required for filopodial activity of the LE.

4.5 Dorsal midline is a busy place during dorsal vessel development

The mature dorsal vessel occupies the space beneath the ectoderm at the dorsal midline. The mesodermally derived CBs have to migrate along the lateral side of the embryo towards the dorsal side. Subsequently to germ band retraction, the ectodermal LE migrates dorsally to the midline to replace the AS and form a continuous ectoderm. The CBs migrate along with the ectodermal LE; however, they are shown to maintain a constant distance away from these cells until the fusion of the ectoderm is complete (Fig 8). Once the fusion of the ectoderm is complete, CBs contact their contralateral partners and lumen formation ensues. The AS is internalized into the embryo as the ectoderm fuses together. Our cross sectional images demonstrate that even after the ectodermal fusion has occurred, the AS still maintains contact with the ectoderm (Fig 8). Other studies have shown that these cells are internalized by apical constriction, which occurs by shrinkage of the apical domain of the cell as the cells move into the embryo (Kiehart, et al. 2000; Toyama, et al. 2008). We observed the AS cells to have pear shaped morphology with DE-Cadherin localized to the apical side of the cell which is oriented towards the overlaying ectoderm (Fig 7,8). In cross sectional EM images of fixed embryo, the localization of AS, CBs and ectoderm was demonstrated (Fig 7,8). Due to this we asked the question how does heart development occur with the AS cells occupying the midline? And what is the relative localization of these cell types during heart development? To answer these questions we labelled all three tissues in live embryos and observed their localization relative to one another during late stages of heart development when all the cells are in close proximity to the midline.

The internalization of the AS occurs at the late stages of DC. AS is internalized through the midline into the embryo where AS cells undergo apoptosis, which is triggered due to loss of apical contact with the ectoderm (Nilufar Mohseni, Reed lab personal communication). The AS contacts both CBs and Ectodermal LE cells (Muliyil, et al. 2011). The CBs on the other hand migrate underneath and adjacent to the ectoderm. The contact between these tissues is observed to be maintained throughout heart development (Fig 8). One interesting observation was that AS cells needed to lose contact with the ectoderm for the heart cells to come with in contact with contralateral partners. In support of this, we observed the extension of filopodial processes specifically at the dorsal apical side of the cell which were oriented towards attachement site of AS and ectodermal cells (Fig 7,8). This means that there must be some signal which results in this limited extension of filopodia at the apical side. One explanation for this observation might be that since AS cells contact the apical side of the CB, they somehow inhibit the extension of filopodia. The increase in the filopodial activity on the other hand might be explained by the presence of diffusible molecules that trigger this increase in activity. Possibly apoptotic AS cells are able to release these molecules.

Overall, ectodermal, AS and CB cells occupy the dorsal midline during stage 16 and 17. The interaction between the ectodermal LE cells and AS cells is shown to be required for the proper embryogenesis (Jacinto, et al. 2002). However, the interaction between CB and AS has not been well characterized. We demonstrated that the interaction between these tissues exists. I suspect that this interaction plays a crucial role in both CB migration and lumen formation.

4.6 Conclusion and Future Directions

The work presented here demonstrates the wild-type nature of the migrating CB which actively extends numerous filopodia along with lamellopodia during late stages of dorsal vessel development. These filopodia which in other systems have been shown to participate in cell target recognition, are demonstrated to differentiate between contralateral and non-contralateral partner cells. In other systems, such as the ectodermal LE, filopodia are responsible for zippering of the cells to form a continuous ectoderm. Study by Millard et al. demonstrated that filopodia from the cell are segmentally patterned and can only recognize cells on the other row which are from the same segment (Millard and Martin. 2008). It is not known how the CBs are able to precisely recognize their contralateral parnters however it might be possible that filopodia are able to differentiate between *svp* and *tinman* expressing cells.

During CNS development Slit and Robo are required for the repulsive forces at the LE of growth cones. However another receptor-ligand pair, Frizzled and Netrin, is required for attractive axon guidance during CNS development and plays an antagonistic role to Slit/Robo (Harris, et al. 1996). Netrin and its receptor Frizzled are required. Additionally, in salivary gland development, both Slit/Robo and Netrin/Frizzled signalling was shown to be required for the correct orientation of salivary gland lobes (Kolesnikov and Beckendorf, 2005). Since the requirement for Robo/Slit was demonstrated in heart development and salivary gland along with Netrin/Frizzled, it might be possible that Netrin/Frizzled also plays a role in attractive CB guidance to the midline. However, the source of Netrin is not yet known. Since the internalizing AS is

located at the dorsal midline (the future site of the dorsal vessel), it might be possible that AS cells are the main source of Netrin.

Another possible source of guidance molecules might be the ectodermal LE. Results show that ectodermal LE migrate ahead of the CB and maintain a steady distance. Based on this I propose two models of CB migration. First model states that it might be possible for ectodermal LE cells to leave a guidance trail for the CB to follow to the midline. If this is true, CBs are expected to follow the trailing edge of the DME cells and never migrate past these cells. This observation holds true in live embryos demonstrated by cross-sectional analysis of the embryos (Fig 8). On the other hand, at stage 15, CB extensions at the LE are able to contact the basal part of the ectodermal LE cells (Fig 2). Since the same observation holds true in live embryos (Fig 8), it might be possible that CBs migrate by direct association with the ectoderm or the DME cells. In favour of the second model, we observe the filopodial processes from CB to be extended at the domain of the cells which is closest to the DME cell. This extension might be present due to a signal from the ectoderm.

Future experiments, which will focus on interaction of CBs with surrounding tissue, will be required to fully understand the migration and polarization pattern of CBs. In addition to Robo/Slit signalling, the role of other signalling system must be explored in this process. With the help of these experiments we might get a little closer to understanding heart development.

References

Albrecht, S., Wang, S., Holz, A., Bergter, A., Paululat, A., 2006. The ADAM Metalloprotease Kuzbanian is Crucial for Proper Heart Formation in Drosophila Melanogaster. Mech Dev 123, 372-387.

Battye, R., Stevens, A., and Jacobs, J.R. 1999. Axon repulsion from the midline of the Drosophila CNS requires slit function. Development 126, 2475-2481.

Bashaw, G.J., Kidd, T., Murray, D., Pawson, T., Goodman, C.S., 2000. Repulsive Axon Guidance: Abelson and Enabled Play Opposing Roles Downstream of the Roundabout Receptor. Cell 101, 703-715.

Bashaw, G.J., Goodman, C.S., 1999. Chimeric Axon Guidance Receptors: The Cytoplasmic Domains of Slit and Netrin Receptors Specify Attraction Versus Repulsion. Cell 97, 917-926.

Bier, E., Bodmer, R., 2004. Drosophila, an Emerging Model for Cardiac Disease. Gene 342, 1-11.

Bodmer, R., Venkatesh, T.V., 1998. Heart Development in Drosophila and Vertebrates: Conservation of Molecular Mechanisms. Dev Genet 22, 181-186.

Brose, K., Bland, K.S., Wang, K.H., Arnott, D., Henzel, W., Goodman, C.S., Tessier-Lavigne, M., Kidd, T., 1999. Slit Proteins Bind Robo Receptors and have an Evolutionarily Conserved Role in Repulsive Axon Guidance. Cell 96, 795-806.

Chen, J.N., Fishman, M.C., 2000. Genetics of Heart Development. Trends Genet 16, 383-388.

Coleman, H.A., Labrador, J.P., Chance, R.K., Bashaw, G.J., 2010. The Adam Family Metalloprotease Kuzbanian Regulates the Cleavage of the Roundabout Receptor to Control Axon Repulsion at the Midline. Development 137, 2417-2426.

Dickson, B.J., Gilestro, G.F., 2006. Regulation of Commissural Axon Pathfinding by Slit and its Robo Receptors. Annu Rev Cell Dev Biol 22, 651-675.

Dimitrova, S., Reissaus, A., Tavosanis, G., 2008. Slit and Robo Regulate Dendrite Branching and Elongation of Space-Filling Neurons in Drosophila. Dev Biol 324, 18-30.

Edwards, K.A., Demsky, M., Montague, R.A., Weymouth, N., Kiehart, D.P., 1997. GFP-Moesin Illuminates Actin Cytoskeleton Dynamics in Living Tissue and

Demonstrates Cell Shape Changes during Morphogenesis in Drosophila. Dev Biol 191, 103-117.

Englund, C., Steneberg, P., Falileeva, L., Xylourgidis, N., Samakovlis, C., 2002. Attractive and Repulsive Functions of Slit are Mediated by Different Receptors in the Drosophila Trachea. Development 129, 4941-4951.

Galbraith, C.G., Yamada, K.M., Galbraith, J.A., 2007. Polymerizing Actin Fibers Position Integrins Primed to Probe for Adhesion Sites. Science 315, 992-995.

Ghose, A., Van Vactor, D., 2002. GAPs in Slit-Robo Signaling. Bioessays 24, 401-404.

Harris, R., Sabatelli, L.M., Seeger, M.A., 1996. Guidance Cues at the Drosophila CNS Midline: Identification and Characterization of Two Drosophila Netrin/UNC-6 Homologs. Neuron 17, 217-228.

Hartenstein V, Jan Y. 1992. Studying Drosophila embryogenesis with P-lacZ enhancer trap lines. Rouxs Arch Dev Biol 201: 194–220.

Hartenstein, V. 1993. Atlas of Drosophila Development. Cold Spring Harbor Laboratory Press. pg 46-47. (http://www.sdbonline.org/fly/atlas/4647.htm)

Heisenberg, C.P., 2009. Dorsal Closure in Drosophila: Cells Cannot Get Out of the Tight Spot. Bioessays 31, 1284-1287.

Helenius, I.T., Beitel, G.J., 2008. The First "Slit" is the Deepest: The Secret to a Hollow Heart. J Cell Biol 182, 221-223.

Hoffman, J.I., 1995. Incidence of Congenital Heart Disease: I. Postnatal Incidence. Pediatr Cardiol 16, 103-113.

Hohenester, E., 2008. Structural Insight into Slit-Robo Signalling. Biochem Soc Trans 36, 251-256.

Jacinto, A., Woolner, S., Martin, P., 2002. Dynamic Analysis of Dorsal Closure in Drosophila: From Genetics to Cell Biology. Dev Cell 3, 9-19.

Johnson, K.G., Ghose, A., Epstein, E., Lincecum, J., O'Connor, M.B., Van Vactor, D., 2004. Axonal Heparan Sulfate Proteoglycans Regulate the Distribution and Efficiency of the Repellent Slit during Midline Axon Guidance. Curr Biol 14, 499-504.

Kadam, S., McMahon, A., Tzou, P., Stathopoulos, A., 2009. FGF Ligands in Drosophila have Distinct Activities Required to Support Cell Migration and Differentiation. Development 136, 739-747.

Keshishian, H., Broadie, K., Chiba, A., Bate, M., 1996. The Drosophila Neuromuscular Junction: A Model System for Studying Synaptic Development and Function. Annu Rev Neurosci 19, 545-575.

Kidd, T., Bland, K.S., Goodman, C.S., 1999. Slit is the Midline Repellent for the Robo Receptor in Drosophila. Cell 96, 785-794.

Kidd, T., Brose, K., Mitchell, K.J., Fetter, R.D., Tessier-Lavigne, M., Goodman, C.S., Tear, G., 1998. Roundabout Controls Axon Crossing of the CNS Midline and Defines a Novel Subfamily of Evolutionarily Conserved Guidance Receptors. Cell 92, 205-215.

Kiehart, D.P., Galbraith, C.G., Edwards, K.A., Rickoll, W.L., Montague, R.A., 2000. Multiple Forces Contribute to Cell Sheet Morphogenesis for Dorsal Closure in Drosophila. J Cell Biol 149, 471-490.

Klingseisen, A., Clark, I.B., Gryzik, T., Muller, H.A., 2009. Differential and Overlapping Functions of Two Closely Related Drosophila FGF8-Like Growth Factors in Mesoderm Development. Development 136, 2393-2402.

Knox, J., Moyer, K., Yacoub, N., Soldaat, C., Komosa, M., Vassilieva, K., Wilk, R., Hu, J., Vazquez Paz Lde, L., Syed, Q., Krause, H.M., Georgescu, M., Jacobs, J.R., 2011. Syndecan Contributes to Heart Cell Specification and Lumen Formation during Drosophila Cardiogenesis. Dev Biol 356, 279-290.

Kohsaka, H., Nose, A., 2009. Target Recognition at the Tips of Postsynaptic Filopodia: Accumulation and Function of Capricious. Development 136, 1127-1135.

Kolesnikov, T., Beckendorf, S.K., 2005. NETRIN and SLIT Guide Salivary Gland Migration. Dev Biol 284, 102-111.

Lieber, T., Kidd, S., Young, M.W., 2002. Kuzbanian-Mediated Cleavage of Drosophila Notch. Genes Dev 16, 209-221.

Liu, Z., Patel, K., Schmidt, H., Andrews, W., Pini, A., Sundaresan, V., 2004. Extracellular Ig Domains 1 and 2 of Robo are Important for Ligand (Slit) Binding. Mol Cell Neurosci 26, 232-240.

MacMullin, A., Jacobs, J.R., 2006. Slit Coordinates Cardiac Morphogenesis in Drosophila. Dev Biol 293, 154-164.

Martin, P.

Medioni, C., Astier, M., Zmojdzian, M., Jagla, K., Semeriva, M., 2008. Genetic Control of Cell Morphogenesis during Drosophila Melanogaster Cardiac Tube Formation. J Cell Biol 182, 249-261.

Millard, T.H., Martin, P., 2008. Dynamic Analysis of Filopodial Interactions during the Zippering Phase of Drosophila Dorsal Closure. Development 135, 621-626.

Muliyil, S.,Krishnakumar, P.,Narasimha, M. 2011. Spatial, temporal and molecular hierarchies in the link between dealth, delamination and dorsal closure. Development 138, 3043-3054.

Murray, M.J., Whitington, P.M., 1999. Effects of Roundabout on Growth Cone Dynamics, Filopodial Length, and Growth Cone Morphology at the Midline and Throughout the Neuropile. J Neurosci 19, 7901-7912.

Poelmann, R.E., Gittenberger-de Groot, A.C., 2005. Apoptosis as an Instrument in Cardiovascular Development. Birth Defects Res C Embryo Today 75, 305-313.

Qian, L., Liu, J., Bodmer, R., 2005. Slit and Robo Control Cardiac Cell Polarity and Morphogenesis. Curr Biol 15, 2271-2278.

Reed, B.H., McMillan, S.C., Chaudhary, R. 2009. The Preparation of Drosophila Embryos for Live-Imaging Using the Hanging Drop Protocol. J. Vis. Exp. 25, e1206, DOI: 10.3791/1206 (2009)

Reed, B.H., Wilk, R., Schock, F., Lipshitz, H.D., 2004. Integrin-Dependent Apposition of Drosophila Extraembryonic Membranes Promotes Morphogenesis and Prevents Anoikis. Curr Biol 14, 372-380.

Rooke, J., Pan, D., Xu, T., Rubin, G.M., 1996. KUZ, a Conserved Metalloprotease-Disintegrin Protein with Two Roles in Drosophila Neurogenesis. Science 273, 1227-1231.

Rothberg, J.M., Jacobs, J.R., Goodman, C.S., Artavanis-Tsakonas, S., 1990. Slit: An Extracellular Protein Necessary for Development of Midline Glia and Commissural Axon Pathways Contains both EGF and LRR Domains. Genes Dev 4, 2169-2187.

Santiago-Martinez, E., Soplop, N.H., Patel, R., Kramer, S.G., 2008. Repulsion by Slit and Roundabout Prevents Shotgun/E-Cadherin-Mediated Cell Adhesion during Drosophila Heart Tube Lumen Formation. J Cell Biol 182, 241-248.

Santiago-Martinez, E., Soplop, N.H., Kramer, S.G., 2006. Lateral Positioning at the Dorsal Midline: Slit and Roundabout Receptors Guide Drosophila Heart Cell Migration. Proc Natl Acad Sci U S A 103, 12441-12446.

Scuderi A, Letsou A. 2005. Amnioserosa is required for dorsal closure in Drosophila. Dev Dyn 232: 791–800.

Seeger, M., Tear, G., Ferres-Marco, D., Goodman, C.S., 1993. Mutations Affecting Growth Cone Guidance in Drosophila: Genes Necessary for Guidance Toward Or Away from the Midline. Neuron 10, 409-426.

Tao, Y., Schulz, R.A., 2007. Heart Development in Drosophila. Semin Cell Dev Biol 18, 3-15.

Toyama, Y., Peralta, X.G., Wells, A.R., Kiehart, D.P., Edwards, G.S., 2008. Apoptotic Force and Tissue Dynamics during Drosophila Embryogenesis. Science 321, 1683-1686.

Tucker, P.K., Evans, I.R., Wood, W., 2011. Ena Drives Invasive Macrophage Migration in Drosophila Embryos. Dis Model Mech 4, 126-134.

Zaffran, S., Frasch, M., 2002. Early Signals in Cardiac Development. Circ Res 91, 457-469.

Zhang, C., Tian, L., Chi, C., Wu, X., Yang, X., Han, M., Xu, T., Zhuang, Y., Deng, K., 2010. Adam10 is Essential for Early Embryonic Cardiovascular Development. Dev Dyn 239, 2594-2602.

APPENDIX

Supplementary Data

Figure 12. Down regulation of s*lit* via dsRNA expression in *svp* cells. (A-A'') Images of embryos stained with anti-Slit and anti-Dmef antibodies are shown below. At late stage of dorsal vessel development Slit localizes to the apical domain of all the CB. (A-A') Both *svp* and *tinman* expressing cells secrete Slit molecule from the apical side which is required for the formation of the lumen. (A'') A zoom-in view of the CB shows that 6 consecutive ipsilateral cells (*svp* and *tinman* cells) have Slit localized to their apical domain. (B-B') When *slit* is down regulated in *svp* cells by the expression of dsRNA construct under the control of *svpGAL4*, apical localization of Slit is absent in some cells. The absence also appears to follow a segmental pattern which suggest that reduction of apical Slit is achieved in *svp* cells only since in the neighbouring cells (4 *tinman* cells) Slit apicalization is achieved. (B'') A zoom-in view of a segment shows the absence of Slit labelling in *svp* cells compared to *tinman* cells. Images were recorded and provided by Kendall Dutchak.

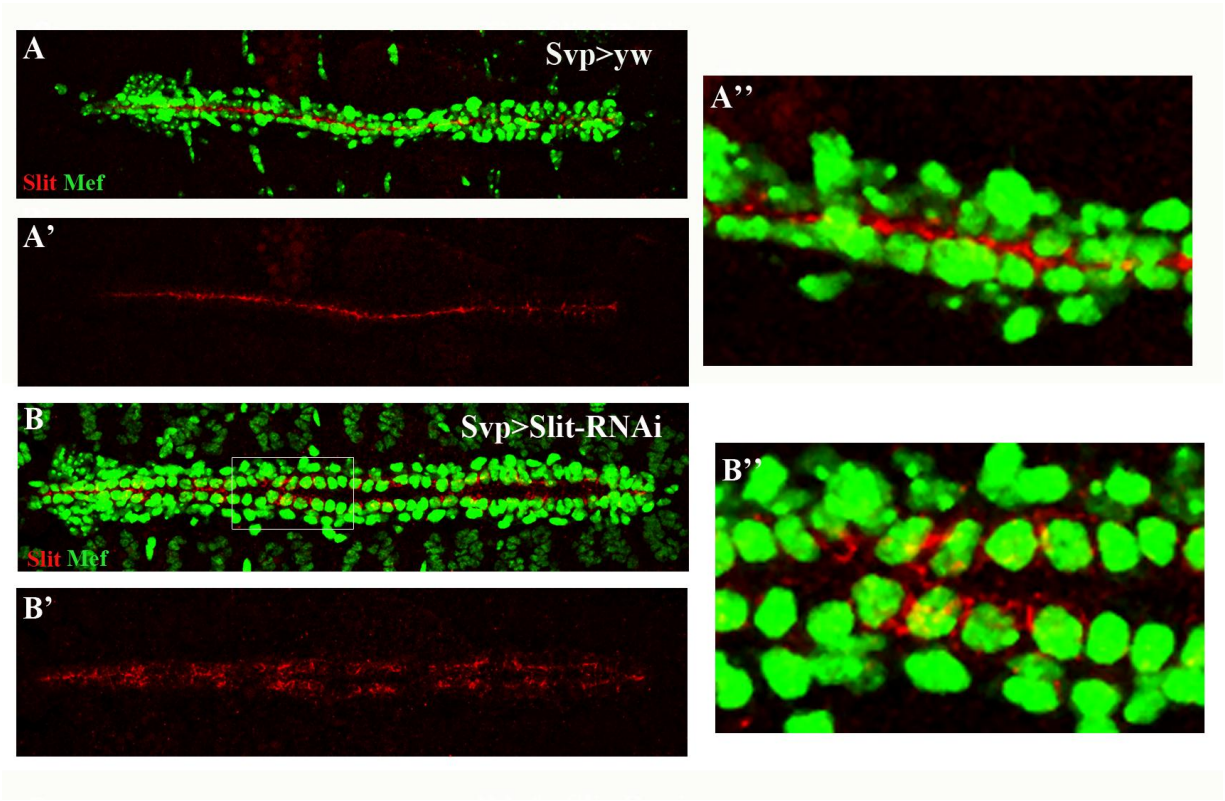
A
Svp>yw
Slit Mef
A'
A''
B
Svp>Slit-RNAi
Slit Mef
B'
B''

Figure 13. *e-cadherin* down regulation via dsRNA expression does not affect filopodial activity. (A-A’’’) Images taken from time-lapse movies of embryos expressing UAS-*moesin-mcherry* under the control of *dmefGAL4* promoter are shown below. Embryos extend filopodial processes at the continuous LE of the CBs. Filopodial activity increases as the bilateral rows migrate closer to the midline. (B-B’’’) Images taken embryos expressing *UAS-moesin-mcherry* and *cad-dsRNA* construct under the control of *dmefGAL4* promoter. The filopodial activity appears to resemble wild-type filopodial activity. A gap spanning two cell diameters was observed on the top bilateral row (arrows).

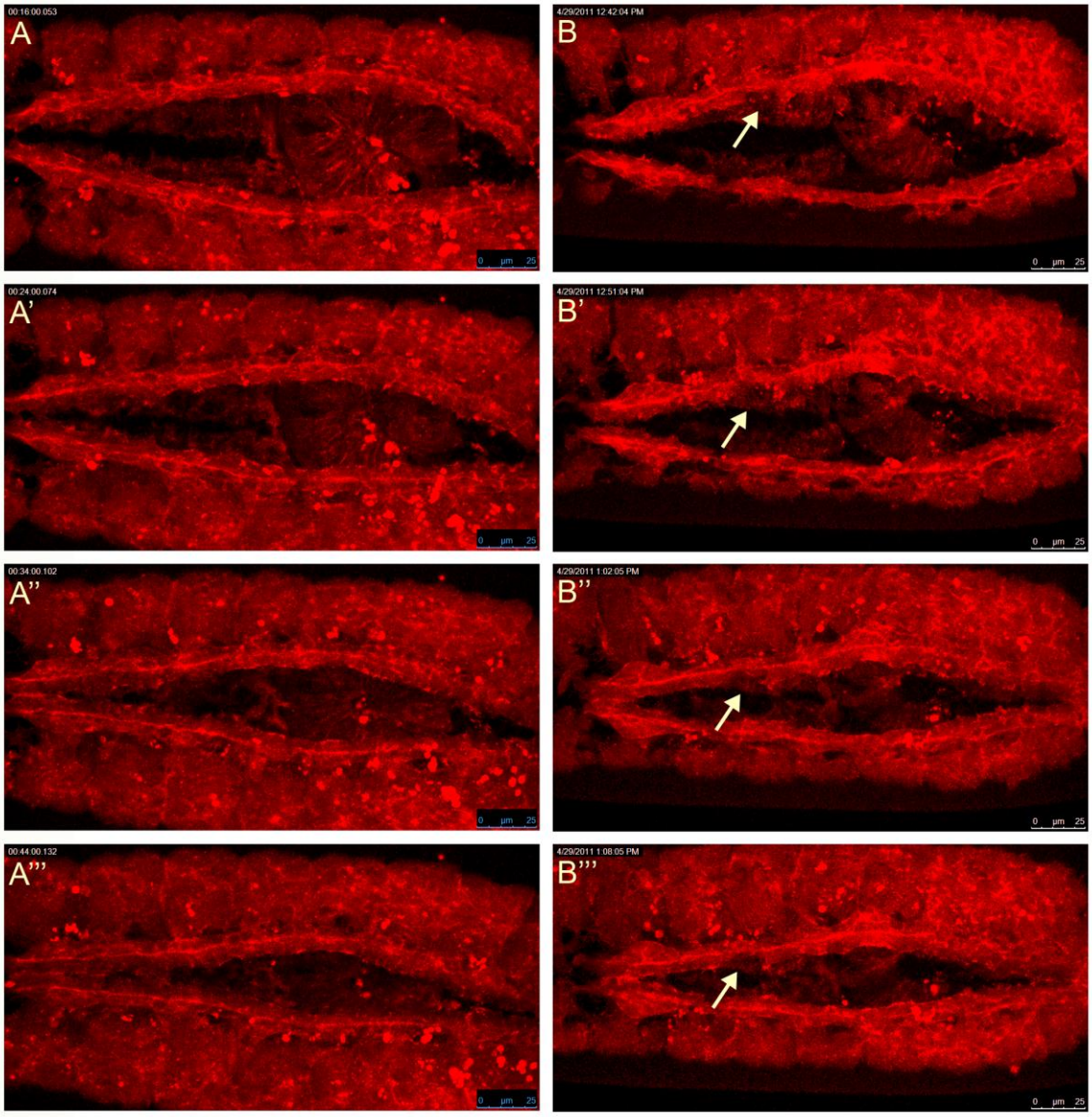
00:16:00.053
A
4/29/2011 12:42:04 PM
B
00:24:00.074
A'
4/29/2011 12:51:04 PM
B'
00:34:00.102
A''
4/29/2011 1:02:05 PM
B''
00:44:00.132
A'''
4/29/2011 1:08:05 PM
B'''
0 µm 25

Figure 14. Contact between ipsilateral cells of the CB in *slit* down regulated embryos. Images taken from time-lapse movies of embryos expressing *UAS-moesin-mcherry* and *slit-dsRNA* constructs under the control of *dmefGAL4* are shown below. A gap spanning one cell diameter is observed in both the top and bottom bilateral (arrowheads). Although the CBs are missing from the LE, the neighbouring CBs extend filopodial processes towards the contralateral partners resembling wild-type behaviour. Neighbouring CBs encompassing the gaps extend filopodial processes into the gap and contact ipsilateral cells. This contact is not maintained and is disrupted (arrows). Scale bar is 25μm.

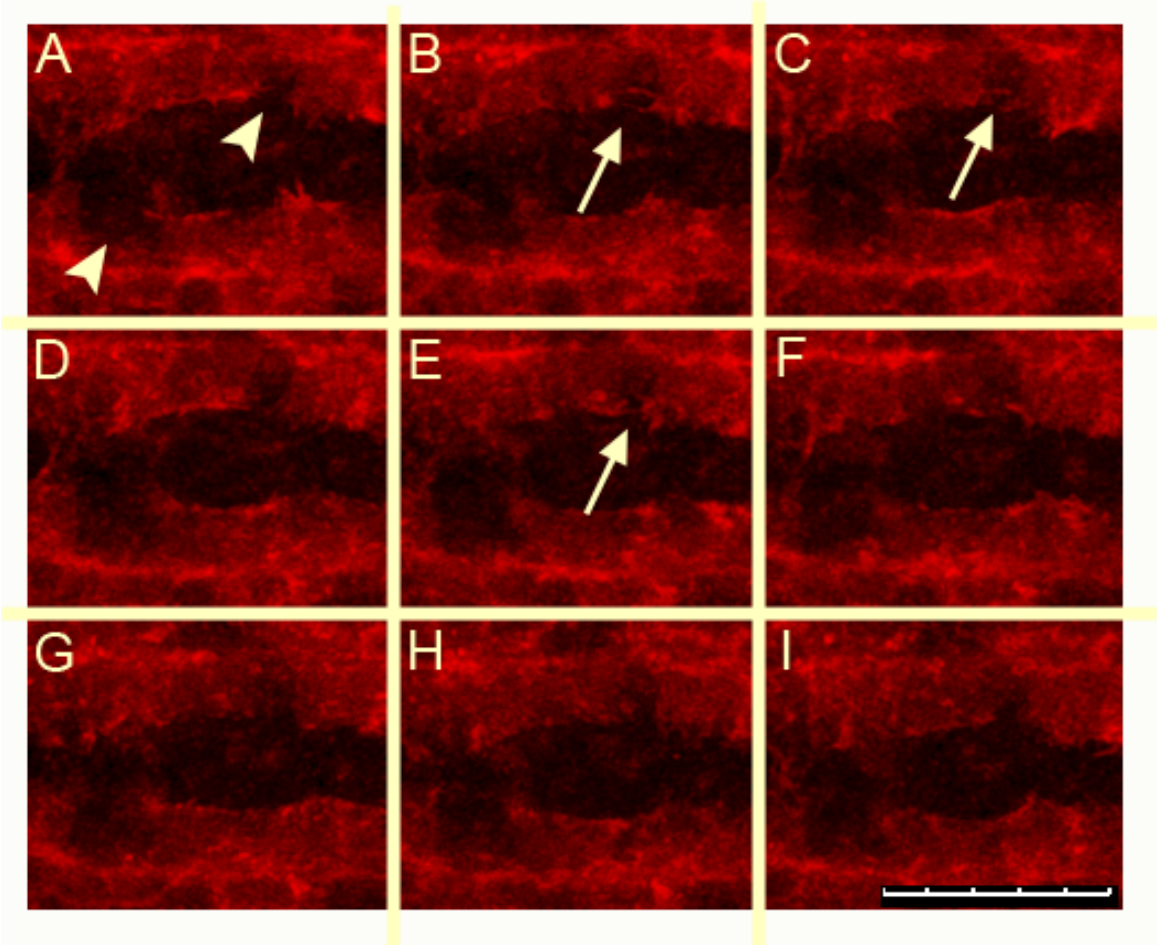
A
B
C
D
E
F
G
H
I